

Calculation of the α -Particle Ground State within the Hyperspherical Harmonic Basis

M. Viviani¹, A. Kievsky¹ and S. Rosati^{1,2}

¹*Istituto Nazionale di Fisica Nucleare, Via Buonarroti 2, 56100 Pisa, Italy and*

²*Dipartimento di Fisica, Universita' di Pisa, Via Buonarroti 2, 56100 Pisa, Italy*

(Dated: July 5, 2018)

The problem of calculating the four-nucleon bound state properties for the case of realistic two- and three-body nuclear potentials is studied using the hyperspherical harmonic (HH) approach. A careful analysis of the convergence of different classes of HH functions has been performed. A restricted basis is chosen to allow for accurate estimates of the binding energy and other properties of the ${}^4\text{He}$ ground state. Results for various modern two-nucleon and two- plus three-nucleon interactions are presented. The ${}^4\text{He}$ asymptotic normalization constants for separation in 2+2 and 1+3 clusters are also computed.

I. INTRODUCTION

Rapid progress has been made during the last few years in the quantitative study of the $A = 4$ nuclear systems. Ever increasing computer power, development of novel numerical methods, and significant refinements of well-established techniques have allowed the solution of the four-nucleon bound state problem with a control of the numerical error at the level of 10-20 keV (the experimental α -particle binding energy (BE) being 28.30 MeV), at least for Hamiltonians including only nucleon-nucleon (NN) interaction models [1]. In the latter work, the BE and other properties of the α -particle were studied with the AV8' [2] NN interaction, and the different techniques produced results in very close agreement with each other (at the level of less than 1%).

In Refs. [3, 4], realistic potential models have been used to describe the α -particle bound state. Those potential models consist of the sum of a modern NN interaction plus a three-nucleon (3N) interaction. A modern NN interaction has the property of describing the NN database with a χ^2 per datum close to one. Examples are the Argonne V18 (AV18) potential [5], the Nijmegen potentials [6], the CD-Bonn potential [7, 8] and the recently proposed potential, non-local in r -space, developed by Doleschall and coll. [9, 10]. This last potential has the remarkable property of reproducing simultaneously the NN bound and scattering data and the 3N binding energies. As is well known, the other models (AV18, Nijmegen and CD-Bonn) underbind the 3N system. Usually a 3N interaction is included in the Hamiltonian when these potentials are considered. The strength of the 3N interaction is properly tuned to reproduce the ${}^3\text{H}$ binding energy and this strength depends on the chosen NN potential. Examples of 3N interactions are the Urbana IX (UIX) [2], the Tucson-Melbourne (TM) [11] and Brazil [12] potentials. From Ref. [3] we observe that all the NN+3N potential models which reproduce the deuteron and the 3N binding energies slightly overbind the α -particle. We further observe that the results obtained using different techniques [3, 4] for the AV18+UIX potential model though close to each other are not in complete agreement. Clearly a clarification of these points would be welcome. Moreover, in recent years there has been a rapid progress in developing new models of the nuclear interaction based on the application of the chiral perturbation theory [13, 14, 15]. From these studies one can hope to have a better understanding of the form of the NN and 3N interactions (the four-nucleon force is expected to be very small). All these potential models have to be studied in detail in the $A = 3$ and $A = 4$ systems. It is therefore very important to have powerful techniques for solving four-nucleon problems.

The methods devised to tackle the problem of the solution of the non-relativistic Schrödinger equation

$$H\Psi(1, 2, 3, 4) = E\Psi(1, 2, 3, 4), \quad (1.1)$$

where H is the four-body nuclear Hamiltonian, are very different. In the Faddeev–Yakubovsky (FY) approach [3, 16, 17, 18], Eq. (1.1) is transformed to a set of coupled equations for the FY amplitudes, which are then solved directly (in momentum or coordinate space) after a partial wave expansion. In the Green Function Monte Carlo (GFMC) method [4, 19] one computes $\exp(-\tau H)\Phi(1, 2, 3, 4)$, where $\Phi(1, 2, 3, 4)$ is a trial wave function (WF), using a stochastic procedure to obtain, in the limit of large τ , the exact ground state WF Ψ . These two techniques have also been applied to the case where the nuclear Hamiltonians includes a 3N interaction. The Stochastic Variational Method (SVM) [20, 21] and the Coupled Rearrangement Channel Gaussian-Basis method (CRCG) [22, 23] provide a variational solution of Eq. (1.1) by expanding the (radial part of the) WF in gaussians. The two techniques differ in the way they determine the non-linear coefficients of the expansion: in the SVM random choices are used to select the optimum set, whereas in the CRCG technique the non linear coefficients are chosen in geometrical progression in such a way that only a few of them have to be varied. Very recently two other new techniques have been proposed. In the no-core shell model (NCSM) method [24, 25] the calculations are performed using a (translational-invariant) harmonic-oscillator (HO) finite basis P and introducing an effective P -dependent Hamiltonian H_P to replace H in Eq. (1.1).

The operator H_P is constructed so that the solution of the equation $H_P\Psi(P) = E_P\Psi(P)$ provides eigenvalues which quickly converge to the exact ones as P is enlarged. The effective interaction hyperspherical harmonic (EHH) method [26] is based on a similar idea, but the finite basis P is constructed in terms of the hyperspherical harmonic (HH) functions.

In the present work we would like to address the problem of calculating the α -particle properties, using a nuclear Hamiltonian containing modern two- and three-nucleon interactions, by expanding the WF in terms of the HH functions. Our intention is to obtain converged binding energies at the level of 20–30 keV. The motivation is twofold. First we would like to reduce the theoretical error in the determination of the α -particle bound state properties. Second, the HH techniques can also be extended to treating four nucleons scattering states, as has been possible for the $A = 3$ system [27] using a similar technique. This program is currently under way and a preliminary report has been already published [28]. The richness of phenomena in the four nucleon scattering and reactions will be an ideal laboratory for studying and testing newer models of the nuclear interaction.

In an earlier work [29], the authors determined the solution of Eq. (1.1) variationally by expanding the WF in a basis of correlated Hyperspherical Harmonic (CHH) WF's. The space part of such a basis consisted of products of correlation factors F and HH functions. The correlation factors F were chosen so as to take into account the strong correlations induced by the NN potential, especially at short inter-particle distances. The introduction of such factors substantially improved the convergence of the expansion. This made it possible to obtain reasonable estimates for the ground state energy of the α particle and some selected observables in $n - {}^3\text{H}$ and $p - {}^3\text{He}$ elastic scattering using a rather limited basis set [29, 30, 31]. However, due to the complexity of F , the spatial integrations were performed by using quasi-random number techniques. The precision of the required matrix elements was therefore limited, and the inclusion of a greater number of states was problematic.

When the four-nucleon WF is expanded in terms of the uncorrelated HH basis (i.e. setting $F = 1$) most of the integrations can be performed analytically, and the remaining low-dimensional integrals can be evaluated by means of efficient quadrature methods. However, due to the particular structure of the NN potential, which is state dependent and strongly repulsive at short distances, a very large number of basis elements are required. For that reason, the application of the HH technique to studying the $A = 4$ nuclear system has encountered serious convergence problems. Few four-body HH calculations have been attempted so far for realistic interactions [32, 33, 34]. Even for central or super-soft-core potentials the problem of the slow convergence of the HH expansion has not been completely overcome [32, 34, 35]. The reason for these difficulties is related to the slow convergence of the basis with respect to the grand angular quantum number K and to the large number of HH states with a given K . For example, for an accurate description of the α -particle ground state, antisymmetric spin-isospin-HH states up to $K = 60$ have to be included. However, the number of such states already for $K = 20$ is greater than 1,000 and it increases very rapidly with K . It is therefore clear that a *brute force* application of the method is not possible even with sophisticated computational facilities.

The approach analyzed in the past was to select a suitable subset of states [36, 37, 38]. In those papers it resulted quite clearly that the quantum number K is not the unique parameter important for studying the convergence of the basis. Let us recall that a 4-body HH function is specified by three orbital angular momentum quantum numbers ℓ_1, ℓ_2, ℓ_3 and two additional quantum numbers n_2, n_3 (which are non-negative integers) related to the radial excitation of the system. The grand angular quantum number is defined to be $K = \ell_1 + \ell_2 + \ell_3 + 2(n_2 + n_3)$. Note that $\mathcal{L} = \ell_1 + \ell_2 + \ell_3$ and K are even (odd) numbers for positive (negative) parity states. In Ref. [36], the basis was restricted to including HH states with a few choices of ℓ_1, ℓ_2, ℓ_3 values, and large values of n_2 and n_3 . The calculations performed [32, 33] were however limited by the computer power available at that time. In this paper, it is shown that HH states having $\mathcal{L} \equiv \ell_1 + \ell_2 + \ell_3 \leq 6$ are sufficient in order to obtain a four digit convergence. However, the number of HH states with $\mathcal{L} \leq 6$ is still huge and additional criteria for selecting a reduced basis have to be specified.

It is possible to organize the HH states in terms of the number of particles correlated. For example, there is a class of elements which depends only on the coordinate of two particles, the so called Potential Basis (PB) [38]. Such a basis therefore takes the two-body correlations into account. However, even in the case of simple model interactions, the BE's B obtained by restricting the expansion basis to the PB were found to be rather far from the exact values. For example, for the Malfliet-Tjon V (MT-V) central potential [48], B calculated with the PB is approximately 1 MeV smaller than the exact value. For a realistic potential the situation is noticeably worse. However, it is clear that the procedure of classifying the HH states in terms of the number of correlated particles can be useful for distinguishing the importance of the various expansion terms.

In the present paper the application of the HH expansion basis is developed by taking advantage of both strategies discussed above. Namely, HH states of low values of ℓ_1, ℓ_2, ℓ_3 are included first. Among them, those correlating only a particle pair are included first, then those correlating three particles are added and so on. In practice, the HH states are first divided into *classes* depending on the value of \mathcal{L} and n_2, n_3 . Let us denote with $\mathcal{M}_i(K_i)$ the number of states belonging to a class i with $K \leq K_i$. Such a number of states rapidly increases with K_i , in general $\mathcal{M}_i(K_i) \approx M_i(K_i)^r$ for large K_i , where the numbers M_i are a set of constants and $r = 1$ or 2 . The first and most

important classes should contain only a small subset of HH states (“small” classes), namely their M_i should be small, let us say $M_i \approx 1$. It is then relatively easy to include HH states of large K belonging to these classes. The classes containing successively larger numbers of states ($M_i \gg 1$) should be chosen possibly so as to contribute lesser and lesser to the expansion in such a way that the corresponding expansion can be truncated to small values of K . A careful analysis of the convergence properties of the various HH components has allowed for an optimal choice of the classes, so that accurate calculations of the α -particle properties could be achieved.

An important aspect of a successful application of the HH method is related to the computation of the coefficients for the transformation of a HH function corresponding to a generic permutation of the 4 particles in terms of those constructed for a given permutation. Various approaches have been devised to deal with this problem [40, 41, 42, 43, 44, 45]. The usefulness of these coefficients is twofold. First, it is easy to identify the linearly dependent states and to avoid their inclusion in the expansion basis. The removal of these “spurious” states, which disappear after a proper antisymmetrization of the basis, is very useful as the number of linear independent states is noticeably smaller than the full degeneracy of the basis. Secondly, the matrix elements of a local two-body (three-body) potential energy operator are easily reduced to one-dimensional (tri-dimensional) integrations, which can also be performed beforehand and stored on computer disks. The matrix elements of non-local operators can also be reduced to low-dimensional integrals. The kinetic energy operator is easily obtained analytically.

This study is the continuation of the application of the HH expansion to the three nucleon system performed in Ref. [46]. Another possible extension of these studies are related to the application of the HH technique to heavier systems. In particular, we can point out that also for $A > 4$ the calculation of the multidimensional integrals related to the matrix elements of a local NN (3N) interaction reduces to a one-dimensional (three-dimensional) integration. The only difficulty in extending the method to heavier systems is the choice of a suitable and optimized subset of HH functions. We hope that the criteria used here to select an optimal subset of the basis could also be applied for systems with $A > 4$.

This paper is organized as follows. In the next section, a brief description of the properties of the HH functions is reported. In section 3, the choice of the basis is presented. The results obtained for the BE and other properties of the α -particle are presented in Sect.4. Finally, the last section is devoted to the conclusions and the perspectives of the present approach.

II. THE HH EXPANSION

For four equal mass particles, a suitable choice of the Jacobi vectors is

$$\begin{aligned}\xi_{1p} &= \sqrt{\frac{3}{2}}\left(\mathbf{r}_m - \frac{\mathbf{r}_i + \mathbf{r}_j + \mathbf{r}_k}{3}\right), \\ \xi_{2p} &= \sqrt{\frac{4}{3}}\left(\mathbf{r}_k - \frac{\mathbf{r}_i + \mathbf{r}_j}{2}\right), \\ \xi_{3p} &= \mathbf{r}_j - \mathbf{r}_i,\end{aligned}\tag{2.1}$$

where p specifies a given permutation corresponding to the order i, j, k and m of the particles. By definition, the permutation $p = 1$ is chosen to correspond to the order 1, 2, 3 and 4.

For a given choice of the Jacobi vectors, the hyperspherical coordinates are given by the hyperradius ρ , defined by

$$\rho = \sqrt{\xi_{1p}^2 + \xi_{2p}^2 + \xi_{3p}^2}, \quad (\text{independent on } p), \tag{2.2}$$

and by a set of variables which in the Zernike and Brinkman [38, 47] representation are the polar angles $\hat{\xi}_{ip} \equiv (\theta_{ip}, \phi_{ip})$ of each Jacobi vector, and the two additional “hyperspherical” angles φ_{2p} and φ_{3p} defined as

$$\cos \varphi_{2p} = \frac{\xi_{2p}}{\sqrt{\xi_{1p}^2 + \xi_{2p}^2}}, \quad \cos \varphi_{3p} = \frac{\xi_{3p}}{\sqrt{\xi_{1p}^2 + \xi_{2p}^2 + \xi_{3p}^2}} = \frac{\xi_{3p}}{\rho}, \tag{2.3}$$

where ξ_{jp} is the magnitude of the Jacobi vector ξ_{jp} . The set of the variables $\hat{\xi}_{1p}, \hat{\xi}_{2p}, \hat{\xi}_{3p}, \varphi_{2p}, \varphi_{3p}$ is denoted hereafter as Ω_p . To simplify the notation for $p = 1$, the subscript “1” will be sometime omitted. The expression of a generic HH function is

$$\mathcal{Y}_{\ell_1, \ell_2, \ell_3, L_2, n_2, n_3}^{K, LM}(\Omega_p) = \left[\left(Y_{\ell_1}(\hat{\xi}_{1p}) Y_{\ell_2}(\hat{\xi}_{2p}) \right)_{L_2} Y_{\ell_3}(\hat{\xi}_{3p}) \right]_{LM} \mathcal{P}_{n_2, n_3}^{\ell_1, \ell_2, \ell_3}(\varphi_{2p}, \varphi_{3p}), \tag{2.4}$$

where

$$\begin{aligned} \mathcal{P}_{n_2, n_3}^{\ell_1, \ell_2, \ell_3}(\varphi_{2p}, \varphi_{3p}) &= \mathcal{N}_{n_2, n_3}^{\ell_1, \ell_2, \ell_3} \sin^{\ell_1} \varphi_{2p} \cos^{\ell_2} \varphi_{2p} \sin^{\ell_1 + \ell_2 + 2n_2} \varphi_{3p} \cos^{\ell_3} \varphi_{3p} \times \\ &\quad P_{n_2}^{\ell_1 + \frac{1}{2}, \ell_2 + \frac{1}{2}}(\cos 2\varphi_{2p}) P_{n_3}^{\ell_1 + \ell_2 + 2n_2 + 2, \ell_3 + \frac{1}{2}}(\cos 2\varphi_{3p}) , \end{aligned} \quad (2.5)$$

and $P_n^{a,b}$ are Jacobi polynomials. The coefficients $\mathcal{N}_{n_2, n_3}^{\ell_1, \ell_2, \ell_3}$ are normalization factors, given explicitly by

$$\mathcal{N}_{n_2, n_3}^{\ell_1, \ell_2, \ell_3} = \prod_{j=2}^3 \left[\frac{2\nu_j \Gamma(\nu_j - n_j) n_j!}{\Gamma(\nu_j - n_j - \ell_j - 1/2) \Gamma(n_j + \ell_j + 3/2)} \right]^{\frac{1}{2}} , \quad (2.6)$$

where $\nu_j = K_j + (3j - 5)/2$ with K_j defined to be

$$K_2 = \ell_1 + \ell_2 + 2n_2 , \quad K_3 = K_2 + \ell_3 + 2n_3 \equiv K , \quad (2.7)$$

and K is the grand angular quantum number.

The HH functions are eigenfunctions of the hyperangular part of the kinetic energy operator Λ^2 . In fact, for $A = 4$ the latter operator can be written using the variables $\{\rho, \Omega_p\}$ as follows

$$\sum_{j=1,3} \nabla_j^2 = \left[\frac{\partial^2}{\partial \rho^2} + \frac{8}{\rho} \frac{\partial}{\partial \rho} + \frac{\Lambda^2(\Omega_p)}{\rho^2} \right] , \quad (2.8)$$

and

$$\left(\Lambda^2(\Omega_p) + K(K + 7) \right) \mathcal{Y}_{\ell_1, \ell_2, \ell_3, L_2, n_2, n_3}^{K, LM}(\Omega_p) = 0 . \quad (2.9)$$

Another important property of the HH functions is that $\rho^K \mathcal{Y}_{\ell_1, \ell_2, \ell_3, L_2, n_2, n_3}^{K, LM}(\Omega_p)$ are homogeneous polynomials of the particle coordinates of degree K .

The WF of a state with total angular momentum J , parity π and total isospin T can be expanded over the following complete basis of antisymmetrical hyperangular–spin–isospin states, defined as

$$\Psi_\mu^{K L S T J \pi} = \sum_{p=1}^{12} \Phi_\mu^{K L S T J \pi}(i, j; k; m) , \quad (2.10)$$

where the sum is over the 12 even permutations p , and

$$\Phi_\mu^{K L S T J \pi}(i, j; k; m) = \left\{ \mathcal{Y}_{\ell_1, \ell_2, \ell_3, L_2, n_2, n_3}^{K, LM}(\Omega_p) \left[\left[[s_i s_j]_{S_a} s_k \right]_{S_b} s_m \right]_S \right\}_{JJ_z} \left[\left[[t_i t_j]_{T_a} t_k \right]_{T_b} t_m \right]_{TT_z} . \quad (2.11)$$

Here, $\mathcal{Y}_{\ell_1, \ell_2, \ell_3, L_2, n_2, n_3}^{K, LM}(\Omega_p)$ is the HH state defined in Eq. (2.4), and s_i (t_i) denotes the spin (isospin) function of particle i . The total orbital angular momentum L of the HH function is coupled to the total spin S to give a total angular momentum J , J_z . The quantum number T specifies the total isospin, while $\pi = (-1)^{\ell_1 + \ell_2 + \ell_3}$ is the parity of the state. The integer index μ labels the possible choices of hyperangular, spin and isospin quantum numbers, namely

$$\mu \equiv \{\ell_1, \ell_2, \ell_3, L_2, n_2, n_3, S_a, S_b, T_a, T_b\} , \quad (2.12)$$

compatible with the given values of K, L, S, T, J and π . Another important classification of the states is to group them into “channels”: states belonging to the same channel have the same values of angular $\ell_1, \ell_2, \ell_3, L_2, L$, spin S_a, S_b, S and isospin T_a, T_b, T quantum numbers but different values of n_2, n_3 .

Each state $\Psi_\mu^{K L S T J \pi}$ entering the expansion of the four-nucleon WF must to be antisymmetric under the exchange of any pair of particles. Consequently, it is necessary to consider states such that

$$\Phi_\mu^{K L S T J \pi}(i, j; k; m) = -\Phi_\mu^{K L S T J \pi}(j, i; k; m) . \quad (2.13)$$

Under the exchange $i \leftrightarrow j$, the Jacobi vector ξ_{3p} changes its sign, whereas ξ_{1p} and ξ_{2p} remain unchanged, and, therefore, the HH function $\mathcal{Y}_{\ell_1, \ell_2, \ell_3, L_2, n_2, n_3}^{K, LM}(\Omega_p)$ transforms into itself times a factor $(-1)^{\ell_3}$ (see Eqs. (2.1) and (2.4)). On the other hand, the spin–isospin part transforms into itself times a factor $(-1)^{S_a + T_a}$ for the $i \leftrightarrow j$ exchange. Thus, the condition (2.13) is fulfilled when

$$\ell_3 + S_a + T_a = \text{odd} . \quad (2.14)$$

The number $M_{KLSJT\pi}$ of the antisymmetrical functions $\Psi_{\mu}^{KLSJT\pi}$ having given K, L, S, T, J and π values but different combination of the quantum numbers μ is in general very large. In addition to the degeneracy $N_{KL\pi}$ of the HH basis, the four spins (isospins) can be coupled in different ways to S (T). However, many of the states $\Psi_{\mu}^{KLSJT\pi}$ are linearly dependent amongst themselves. In the expansion of a four-nucleon WF it is necessary to include the subset of linearly independent states only. To search for the independent states, the essential ingredient is the knowledge of

$$N_{\mu\mu'}^{KLSJT\pi} = \langle \Psi_{\mu}^{KLSJT\pi} | \Psi_{\mu'}^{KLSJT\pi} \rangle_{\Omega} , \quad (2.15)$$

where $\langle \rangle_{\Omega}$ denotes the evaluation of the spin–isospin traces and the integration over the hyperspherical variables.

The calculation of the matrix elements of the Hamiltonian is considerably simplified by using the following transformation

$$\Phi_{\mu}^{KLSJT\pi}(i, j; k; m) = \sum_{\mu'} a_{\mu, \mu'}^{KLSJT\pi}(p) \Phi_{\mu'}^{KLSJT\pi}(1, 2; 3; 4) . \quad (2.16)$$

The coefficients $a_{\mu, \mu'}^{KLSJT\pi}(p)$ have been obtained using the techniques described in Ref. [45]. The states $\Psi_{\mu}^{KLSJT\pi}$ can be written as

$$\Psi_{\mu}^{KLSJT\pi} = \sum_{\mu'} A_{\mu, \mu'}^{KLSJT\pi} \Phi_{\mu'}^{KLSJT\pi}(1, 2; 3; 4) , \quad (2.17)$$

where

$$A_{\mu, \mu'}^{KLSJT\pi} = \sum_{p=1}^{12} a_{\mu, \mu'}^{KLSJT\pi}(p) . \quad (2.18)$$

The matrix elements of the norm can be easily obtained using the orthonormalization of the HH basis with the result that:

$$N_{\mu\mu'}^{KLSJT\pi} = \sum_{\mu''} (A_{\mu, \mu''}^{KLSJT\pi})^* A_{\mu', \mu''}^{KLSJT\pi} . \quad (2.19)$$

Clearly,

$$\langle \Psi_{\mu}^{KLSJT\pi} | \Psi_{\mu'}^{K'L'S'T'J'\pi'} \rangle_{\Omega} = 0 , \quad \text{if } \{KLSJT\pi\} \neq \{K'L'S'T'J'\pi'\} . \quad (2.20)$$

Once the quantities $N_{\mu\mu'}^{KLSJT\pi}$ are calculated, the Gram–Schmidt procedure can be used, for example, to eliminate the linear dependent states between the various $\Psi_{\mu}^{KLSJT\pi}$ functions.

We have found that the number of independent states $M'_{KLSJT\pi}$ for given K, L, S, T, J and π is noticeably smaller than the corresponding value of $M_{KLSJT\pi}$. To give an example, we have reported in Table I a few values of $M_{KLSJT\pi}$ and $M'_{KLSJT\pi}$ for the case $J = 0, T = 0, \pi = +$ corresponding to the ground state of the α -particle. As can be seen from the table, the values of M_{KLL00+} are very large also for moderate values of K , but M'_{KLL00+} are usually much smaller.

The total WF can finally be written as

$$\Psi_4^{J\pi} = \sum_{KLSJT} \sum_{\mu} \frac{u_{KLSJT, \mu}(\rho)}{\rho^4} \Psi_{\mu}^{KLSJT\pi} , \quad (2.21)$$

where the sum is restricted only to the linearly independent states. The expansion coefficients, which depend on the hyperradius, are determined by the Rayleigh–Ritz variational principle. By applying this principle, a set of second order differential equations for the functions $u(\rho)$ are obtained. These equations and the procedure adopted to solve them has been outlined in the appendix of Ref. [46]. In this way, a large number of equation can be solved.

The main problem is the computation of the matrix elements of the Hamiltonian. The kinetic energy operator matrix elements are readily calculated analytically, whereas the matrix elements of a local NN potential can be obtained by one dimensional integrations. To this aim, it is convenient to write the basis in the jj coupling scheme

$$\Psi_{\mu}^{KLSJT\pi} = \sum_{\nu} B_{\mu, \nu}^{KLSJT\pi} \Xi_{\nu}^{KLTJ\pi}(1, 2; 3; 4) , \quad (2.22)$$

where

$$\begin{aligned} \Xi_\nu^{KTJ\pi}(1, 2; 3; 4) = & \left\{ \left[\left(Y_{\ell_3}(\hat{\xi}_3)(s_1 s_2)_{s_a} \right)_{j_3} \left(Y_{\ell_2}(\hat{\xi}_2) s_3 \right)_{j_2} \right]_{J_2} \left(Y_{\ell_1}(\hat{\xi}_1) s_4 \right)_{j_1} \right\}_{JJ_z} \times \\ & \times \left[\left[[t_i t_j]_{T_a} t_k \right]_{T_b} t_m \right]_{TT_z} \mathcal{P}_{n_2, n_3}^{\ell_1, \ell_2, \ell_3}(\varphi_{2p}, \varphi_{3p}) , \end{aligned} \quad (2.23)$$

and $B_{\mu, \nu}^{KLSTJ\pi}$ are related to the coefficients $A_{\mu, \mu'}^{KLSTJ\pi}$ via Wigner 3j and 6j coefficients. Now, the integer index ν labels all possible choices of

$$\nu \equiv \{n_3, \ell_3, S_a, j_3, n_2, \ell_2, j_2, J_2, \ell_1, j_1, T_a, T_b\} , \quad (2.24)$$

compatible with the given values of K, T, J and π .

In terms of the states $\Xi_\nu^{KTJ\pi}(1, 2; 3; 4)$, it is easy to compute the matrix elements of an NN potential. For example, the matrix element of the isospin-conserving part $V_{IC}(1, 2)$ of the NN potential

$$\langle \Xi_\nu^{KTJ\pi}(1, 2; 3; 4) | V_{IC}(1, 2) | \Xi_{\nu'}^{K'T'J\pi}(1, 2; 3; 4) \rangle_\Omega = 0 , \quad (2.25)$$

unless

$$\{j_3, n_2, \ell_2, j_2, J_2, \ell_1, j_1, T_a, T_b, T\} = \{j'_3, n'_2, \ell'_2, j'_2, J'_2, \ell'_1, j'_1, T'_a, T'_b, T'\} . \quad (2.26)$$

If Eq. (2.26) is verified, then

$$\begin{aligned} \langle \Xi_\nu^{KTJ\pi}(1, 2; 3; 4) | V_{IC}(1, 2) | \Xi_{\nu'}^{K'TJ\pi}(1, 2; 3; 4) \rangle_\Omega = \\ = \mathcal{N}_{n_2, n_3}^{\ell_1, \ell_2, \ell_3} \mathcal{N}_{n_2, n'_3}^{\ell'_1, \ell'_2, \ell'_3} \int_0^{\frac{\pi}{2}} d\varphi_3 (\cos \varphi_3)^{2+\ell_3+\ell'_3} (\sin \varphi_3)^{5+2\ell_1+2\ell_2+4n_2} \times \\ \times v_{\ell_3, S_a, \ell'_3, S'_a}^{j_3}(\rho \cos \varphi_3) P_{n_3}^{\ell_1+\ell_2+2n_2+2, \ell_3+\frac{1}{2}}(\cos 2\varphi_3) \times \\ \times P_{n'_3}^{\ell'_1+\ell'_2+2n_2+2, \ell'_3+\frac{1}{2}}(\cos 2\varphi_3) , \end{aligned} \quad (2.27)$$

where $v_{\ell, S, \ell', S'}^j(r)$ is the isospin-conserving part of the NN potential acting between two-body states $^{2S+1}(\ell)_j$ and $^{2S'+1}(\ell')_j$. The one-dimensional integral given in Eq. (2.26) can be computed numerically with high accuracy. The case of the isospin-breaking part of the NN interaction is a generalization of the previous case: now we can have $\{T_a, T_b, T\} \neq \{T'_a, T'_b, T'\}$ as well.

The 3N interaction matrix elements are more difficult to compute and the adopted procedure is detailed in the Appendix.

III. CHOICE OF THE BASIS

The main difficulty of applying the HH technique is the selection of a restricted and effective subset of basis states. In fact, although the number of independent states proves to be much smaller than the degeneracy $M_{KLSTJ\pi}$ of the basis, the brute force application of the method, i.e., the inclusion of all HH states having $K \leq K_M$ in the expansion and then increasing K_M until convergence, would be destined to fail. In fact, due to the strong correlations induced by the NN potential, $K_M \approx 60$ are necessary in order to obtain a good convergence. However, already for values of $K > 20$ it is very difficult to find the linearly independent states via the Gram-Schmidt procedure due to the loss of precision in the orthogonalization procedure.

However, it is possible to separate the HH functions into classes having particular properties and advantageously take into account the fact that the convergence rates of the various classes are rather different. As discussed in the Introduction, we expect that the contribution of the HH functions describing the two-body correlations to be very important [38]. Another criterion adopted is first to consider the HH functions with low values of ℓ_i .

An important quantity in the choice of the classes is $\mathcal{M}_i(K_i)$, namely the number of linearly independent antisymmetrical spin-isospin-HH states $\Psi_\mu^{KLSTJ\pi}$ belonging to a class i and having $K \leq K_i$. Only even parity states have been included in the construction of the α -particle WF, and thus the discussion hereafter will be limited to consider only even values for K_i . In general, for a class i , the value $\mathcal{M}_i(K_i)$ is zero for $K_i < K_i^a$, due to the fact that the linearly-dependent states have been removed from the expansion. For example, as should be clear by inspection of

Table I, there is only one linearly-independent state Ψ_{μ}^{KLS00+} with $K = 0$. If this state is included in the first class, the other classes must have at least $K_i^a = 2$, etc. For $K_i \gg K_i^a$, $\mathcal{M}_i(K_i)$ reaches a sort of “asymptotic” value, given by $\mathcal{M}_i(K_i) \approx M_i(K_i)^{r_i}$. The choice of the classes has clearly to be optimized so that the convergence for the classes with large values of M_i and r_i could be reached for relatively low values of K . The specific values of M_i and r_i are discussed below.

To study the α -particle ground state we have found it very convenient to choose as follows (T is the total isospin):

1. Class C1. In this class the $T = 0$ HH states belonging to the PB are included. For $A = 4$, the PB includes states of the first three channels reported in Table II (the only channels with $\ell_1 = \ell_2 = 0$) with $n_2 = 0$. As can be seen from Eq. (2.4), the corresponding states depends only on $\hat{\xi}_{3p}$ and $\cos \varphi_{3p} = \xi_{3p}/\rho \equiv r_{ij}/\rho$, and therefore contain only two-body correlations. For this class, $K_1^a = 0$. For $K_1 \geq 4$, $\mathcal{M}_1(K_1) = (3/2)K_1$. Then, this is a “small” class. As will be shown in the next Section, this is also the most slowly convergent class, but since $M_1 = (3/2)$ and $r_1 = 1$, it is not difficult to reach the desired degree of accuracy.
2. Class C2. This class includes the $T = 0$ states belonging to the same three channels as those of class C1, but with $n_2 > 0$. These states therefore include also part of the three-body correlations. The first linearly-independent states of this class appear for $K = 4$, therefore $K_2^a = 4$. Moreover, $\mathcal{M}_2(K_2) = (3/4)(K_2)^2 + \mathcal{O}(K_2)$ for $K_2 \gg 1$. This can be considered a “small” class, too, and states up to $K_2 = 40$ have been included in the present calculation without difficulty.
3. Class C3. This class includes the remaining $T = 0$ states of the channels having $\ell_1 + \ell_2 + \ell_3 = 2$. The corresponding 20 possible channels are reported in Table II in rows 4 – 23. In this case $K_3^a = 2$ and $\mathcal{M}_3(K_3) = 5(K_3)^2 + \mathcal{O}(K_3)$ for $K_3 \gg 1$. This is a fairly “large” class, but with the necessary care states with $K_3 \approx 34$ can be still included in the expansion.
4. Class C4. This class includes $T = 0$ states belonging to the channels with $\ell_1 + \ell_2 + \ell_3 = 4$. There are 57 channels of this kind. In this case $K_4^a = 8$ and it follows that $\mathcal{M}_4(K_4) = (57/4)(K_4)^2 + \mathcal{O}(K_4)$ for $K_4 \gg 1$. This is a “large” class, but its contribution to the α -particle BE is, though still sizable, far less important than the first three classes. States of up to $K_4 \approx 28$ have been considered.
5. Class C5. This class includes $T = 0$ states belonging to the channels with $\ell_1 + \ell_2 + \ell_3 = 6$. There are 109 channels of this kind. In this case $K_5^a = 12$ and for $K_5 \gg 1$ we have $\mathcal{M}_5(K_5) = (109/4)(K_5)^2 + \mathcal{O}(K_5)$. This is a very “large” class, but it contributes very little to the α -particle BE, as we shall see. Therefore, we can truncate the expansion already at $K_5 \approx 20$.
6. Class C6. This class includes the states having $T > 0$. We have included in the expansion all the channels of this kind with $\ell_1 + \ell_2 + \ell_3 \leq 2$ (45 channels). In this case $K_6^a = 0$ and for $K_6 \gg 1$ we have $\mathcal{M}_6(K_6) = (45/4)(K_6)^2 + \mathcal{O}(K_6)$. Also the contribution to this class is very tiny.

The states belonging to the classes C2 and C3 describe the most important three-body contributions to the WF. The classes C4 and C5 take into account the remaining three and four body correlations ordered with increasing values of $\ell_1 + \ell_2 + \ell_3$.

The convergence is studied as follows. First, only the states of class C1 with $K \leq K_1$ are included in the expansion and the convergence of the BE is studied as the value of K_1 is increased. Once a satisfactory value of $K_1 = K_{1M}$ is reached, the states of the second class with $K \leq K_2$ are added to the expansion, keeping all the states of the class C1 with $K \leq K_{1M}$. Then K_2 is increased up to K_{2M} in order to reach the desired convergence for the BE. With some extra work, it is possible at this point to optimize the basis by removing some of the $K \leq K_{2M}$ states of class C2 which give very tiny contributions to the BE. The procedure outlined is then repeated for each new class. Our complete calculation includes about 8,000 states.

It should be noticed that in the present calculation only HH functions constructed in terms of the Jacobi vectors given in Eq. (2.1), referred to as the set A, have been considered. As is well known, there is another possible choice, namely

$$\begin{aligned}\xi'_{1p} &= \mathbf{r}_m - \mathbf{r}_k, \\ \xi'_{2p} &= \sqrt{\frac{1}{2}}(\mathbf{r}_k + \mathbf{r}_m - \mathbf{r}_i - \mathbf{r}_j), \\ \xi'_{3p} &= \mathbf{r}_j - \mathbf{r}_i,\end{aligned}\tag{3.1}$$

hereafter referred as the set B of Jacobi vectors. Considering, for example, the α -particle ground state, the HH functions $\mathcal{Y}_{\text{set A}}$ of the set A are more appropriate for describing those contributions to the WF corresponding to

$\{3+1\}$ clustering structures, namely ${}^3\text{He} + n$ or ${}^3\text{H} + p$. The HH functions $\mathcal{Y}_{\text{set B}}$ constructed with the set B, should be more suitable for describing the $\{2+2\}$ clustering structures, such as the $d+d$ configurations. It is rather obvious that the inclusion of HH functions of both sets should speed up the convergence in constructing the full state of the system [23, 29]. If the expansion of the WF is done over only a particular set, those configurations in which other clustering structures are important would be generally described with difficulty and a slow convergence would result.

In the present calculation we have included HH states $\mathcal{Y}_{\text{set A}}$ only, i.e. constructed with the Jacobi vectors of the set A, since this has been found to be sufficient to reach the desired degree of convergence. In fact, the full basis considered (classes C1-C6) is large enough to include all the possible independent states for $K \leq 20$. Additional linearly independent states constructed with the set B would appear only for $K \geq 22$. As will appear clear below, the contribution of states with $K \geq 22$ *not belonging* to classes C1–C3 is rather small. Therefore, in the present calculation it is not necessary to introduce states of the set B. However in the present formalism there would be no particular difficulty in also including states constructed with the set B.

IV. RESULTS FOR THE α PARTICLE GROUND STATE

In this section, the results obtained for the ground state of the α particle are presented. The convergence of the HH expansion in terms of the various classes is examined in Sect. IV A. The results obtained for the BE and other properties for a number of different interaction models are reported in Sect. IV B. The origin of the $T > 0$ components in the α -particle ground state is discussed in Sect. IV C. The effect of the truncation of the NN and 3N interactions is studied in Sect. IV D. Finally, the calculation of the various ${}^4\text{He}$ asymptotic normalization constants is considered in Sect. IV E.

A. Convergence

In order to study the convergence, we have considered three different interaction models frequently used in literature. The first calculation has been performed using the MT-V potential [48], a central spin-independent interaction. The parameters defining this potential can be found in Table I of Ref. [20] and we have used $\hbar^2/m = 41.47 \text{ MeV fm}^2$. This potential has been used for a number of benchmarks. It does not contain any non central components, but it retains a rather strong repulsion at short interparticle distance going like $1/r$. It is therefore rather challenging for a technique where the correlations are not built in. In the second example, we have considered the AV18 potential model [5] which represent a NN interaction in its full richness, with short-range repulsion, tensor and other non-central components, charge symmetry breaking terms, and Coulomb and other electromagnetic interactions. In the third case, we have added to the AV18 potential the Urbana IX model [2] of 3N interaction (AV18+UIX model). For the latter two models we have used $\hbar^2/m = 41.47108 \text{ MeV fm}^2$.

We study the convergence as explained in the previous Section, and the results presented in table III are arranged accordingly. For example, the BE B reported in a row with a given set of values of K_1, \dots, K_6 has been obtained by including in the expansion all the HH functions of class C_i with $K \leq K_i$, $i = 1, \dots, 6$.

For the MT-V potential, we observe a slow convergence of the classes C1 and C2 and fairly large values of K have to be used. On the other side, they give 96% of the total BE. The contributions of the other classes are extremely small. The class C3 increases the BE by an additional 0.08 MeV, and the class C4 by less than 0.01 MeV. Class C5 gives a negligible contribution, and class C6 has not been included in the expansion since for this potential isospin is a good quantum number and there is not any mixing with $T > 0$ components. The final value $B = 31.347 \text{ MeV}$ is in good agreement with the results found in literature, whose “average” has been reported in the last row of Table III. There is approximately 10 keV of missing energy due to the truncation of our expansion as will be discussed at the end of this Subsection.

For the AV18 potential, the first two classes give important contributions but a large amount of BE is still missing. The inclusion of the third class increases the BE by more than 3 MeV but 0.8 MeV are still missing. Since the second and third classes take into account a large part of the contributions of the three body correlations, this means that also the four body correlation are important. These are related to the configurations where the clusterization $2+2$ is important. In our calculation, such configurations are included when the classes C4 and C5 are taken into account. The number of the states of class C4 increases very rapidly with K_4 but fortunately the convergence is reached around $K = 24$. The gained BE is almost 0.8 MeV. There are no linearly independent states of class C5 with $K < 14$ and its contribution is rather small. The convergence is again obtained around $K = 24$, but the gain in energy is only about 0.02 MeV. Since the number of states of this class is very large, for example $\mathcal{M}_6(20) \approx 800$ when confronted with a very tiny gain in BE, a selection of the states has to be performed to save computing time and to avoid loss of numerical precision. For example, all the channels of class C5 with a total orbital angular momentum $L = 0$ have not

been included in the expansion since their contribution is absolutely negligible. With their inclusion the procedure of Ref. [46] for finding the eigenvalue would become numerically instable.

From table III, one can try to estimate the contribution of the states with $\mathcal{L} = \ell_1 + \ell_2 + \ell_3 = 8$. From the previous discussion we have already seen that the states having $\mathcal{L} = 4$ (class C4) contribute by about 0.8 MeV, while the states with $\mathcal{L} = 6$ (class C5) contribute by less than 0.03 MeV. Therefore, the states with $\mathcal{L} = 8$ are expected to give a negligible contribution to the α -particle BE. Finally, the inclusion of states with $T > 0$ (class C6) increases the BE by another 20 keV, approximately.

The convergence rate when considering the UIX 3N interaction is similar to the AV18 case. The corresponding results are reported in the last column of table III (they have been obtained in the approximation described in Subsec. IV D). Since the models most frequently used for the 3N interactions are rather soft at short interparticle distances, the convergence rate of the C1 and C2 classes does not change appreciably. However, the 3N potential has a very strong state dependence and the convergence of the C3-C5 classes are now slightly slower. For example, the gain in BE of the C4 class is about 0.8 MeV without any 3N interactions, and it becomes about 1 MeV when including the 3N interaction. Our final results for the AV18 and AV18+UIX models agree well with the FY results of Ref. [51] reported in the last row of Table III. The convergence properties for other NN and NN+3N potential models has been found rather similar to those showed in Table III.

Finally, let us comment about the convergence rate of the expansion as a function of the maximal grand angular quantum numbers K_i of the various classes of HH states included in our expansion. Previous studies [37, 38, 39, 49] have shown that the trend of convergence toward the exact BE depends primarily on the form of the potential. In particular, for potentials which are given as functions of r_{ij}^2 (as, for example, those given as a sum of gaussians) the increase of BE with K_i diminishes exponentially. On the other hand, for potentials given as a function of r_{ij} (as a sum of exponentials or Yukawians), the increase of BE decreases as $(1/K_m)^p$, where p is a positive integer number. The value of p is smaller for potentials of Yukawa type due to the $1/r$ divergence at the origin, but may depends also on the class of the HH functions whose convergence is studied. It is important to determine the value of K_m at which the convergence starts to behave as stated previously. The asymptotic behavior of the convergence should be reached for HH functions whose kinetic energy $\propto (\hbar^2/m)K(K+7)/\rho_0^2$ is much greater than the BE, where ρ_0 is a value of the hyperradius ρ for which $\Psi(\rho_0)$ can be regarded as small [37]. In our studies, we have found that the asymptotic falling begins for $K_m \approx 30 \div 40$.

In order to study the convergence behavior we have indicated with $B(K_1, K_2, K_3, K_4, K_5, K_6)$ the BE obtained by including in the expansion all the HH states of the class C1 with $K \leq K_1$, all the HH states of the class C2 having $K \leq K_2$, etc. Let us compute

$$\Delta_1(K) = B(K, 0, 0, 0, 0, 0) - B(K-2, 0, 0, 0, 0, 0), \quad (4.1)$$

$$\Delta_2(K) = B(K_{1M}, K, 0, 0, 0, 0) - B(K_{1M}, K-2, 0, 0, 0, 0), \quad K_{1M} = 72, \quad (4.2)$$

$$\Delta_3(K) = B(K_{1M}, K_{2M}, K, 0, 0, 0) - B(K_{1M}, K_{2M}, K-2, 0, 0, 0), \quad K_{1M} = 72, K_{2M} = 40, \quad (4.3)$$

and so on. The values obtained for Δ_i , $i = 1, 3$ are shown in Fig. 1 for the MT-V potential model, together with the curves $(1/K)^p$ for $p = 5$ (the curves have been constrained to fit the high K part of the $\Delta_{1+3}(K)$ values). As can be seen in Fig. 1, all the energy differences Δ_1 , Δ_2 and Δ_3 decrease as $1/K^5$ for $K \geq 20$, approximately. However, for a given K , there is a clear hierarchy $\Delta_1(K) \gg \Delta_2(K) \gg \Delta_3(K)$. Note that there are slight fluctuations in the $\Delta(K)$ as K is increased (this is evident in particular for Δ_3).

The values obtained for Δ_i , $i = 1, 4$ for the AV18 potential are reported in Fig. 2. The decrease of Δ_1 , Δ_3 and Δ_4 clearly follows a law $(1/K)^p$ with $p = 7$. The behavior of the energy difference Δ_2 can be approximated either by a $1/K^6$ or a $1/K^7$ law. The faster decrease of these results compared to the previous case is due to the fact that the AV18 potential does not diverge at the origin, while the MT-V has a $1/r$ divergence. The study of Ref. [37], in fact, predicts a difference of two units in the exponential coefficient for the two cases (Yukawian potentials vs. regular potentials). For fixed K , also for the AV18 we note a systematic hierarchy $\Delta_1(K) \gg \Delta_2(K) \gg \Delta_3(K) \gg \Delta_4(K)$, although less pronounced than in the MT-V case. The same behaviour is observed when the UIX 3N potential is included.

From the observed simple behavior, we can readily estimate the missing BE due to the truncation of the expansion to finite values of $K = \bar{K}$. Let us suppose that the states of class i up to $K = \bar{K}$ have been included and to have computed $\Delta_i(\bar{K})$. Then, the missing BE due to the states with $K = \bar{K} + 2, \bar{K} + 4, \dots$, is given by

$$(\Delta B)_i = c(\bar{K}, p) \Delta_i(\bar{K}), \quad c(\bar{K}, p) = \sum_{K=\bar{K}+2, \bar{K}+4, \dots}^{\infty} \left(\frac{\bar{K}}{K} \right)^p, \quad (4.4)$$

where $c(\bar{K}, p)$ is a numerical coefficient. For example, let us consider the “missing” energy for the Class C1 in the MT-V case. In this case $\bar{K} = 72$ and $p = 5$ and $c(72, 5) = 8.51$. Since $\Delta_1(\bar{K} = 72) = 0.99$ keV, we find that

$\Delta B_1 = 8.4$ keV. Adding this value to $B(72, 0, 0, 0, 0, 0)$ we can extrapolate the BE for the case of the inclusion of the *whole* class C1: $B(72, 0, 0, 0, 0, 0) + (\Delta B)_1 \approx 30.041$ MeV. The BE obtained corresponding to this case (converged PB expansion) has been computed very precisely in Ref. [50] using a “pair-correlated” potential basis (PPB). In such an expansion, each PB function is multiplied by a pair correlation factor and this allows for a very rapid convergence of the expansion. In that paper, we found $B(\text{PPB}) = 30.042$ MeV which agrees very well with the above extrapolated value. To reach such a value, it would be necessary to use $\bar{K} \approx 150$ for the class C1.

For the AV18, we find $c(72, 7) = 5.52$, $\Delta_1(\bar{K} = 72) = 0.24$ keV and therefore $(\Delta B)_1 \approx 1.3$ keV, a rather tiny quantity. Due to the faster convergence for this potential like $1/K^7$, it does not seem necessary to increase K_1 any further in this case.

The “missing” energy of the other classes can be estimated in the same way. However, to estimate the “missing” energy for the whole calculation due to the truncation of the expansion of the first class up to $K \leq K_1$, of the second class up to $K \leq K_2$, etc., we cannot simply add the $(\Delta B)_i$, $i = 1, \dots, 6$ so obtained. The reason is that, for example, the inclusion of the HH states of classes C2, C3, ..., also alters the convergence of class C1, etc. by a small amount. To study the “full” rate of convergence, let us consider

$$\begin{aligned}\bar{\Delta}_1(K) &= B(K, K_{2M}, K_{3M}, K_{4M}, K_{5M}, K_{6M}) - \\ &\quad B(K-2, K_{2M}, K_{3M}, K_{4M}, K_{5M}, K_{6M}) , \\ \bar{\Delta}_2(K) &= B(K_{1M}, K, K_{3M}, K_{4M}, K_{5M}, K_{6M}) - \\ &\quad B(K_{1M}, K-2, K_{3M}, K_{4M}, K_{5M}, K_{6M}) , \\ \bar{\Delta}_3(K) &= B(K_{1M}, K_{2M}, K, K_{4M}, K_{5M}, K_{6M}) - \\ &\quad B(K_{1M}, K_{2M}, K-2, K_{4M}, K_{5M}, K_{6M}) ,\end{aligned}\tag{4.5}$$

and so on. Clearly $\Delta_6(K) \equiv \bar{\Delta}_6(K)$. The differences between $\Delta_i(K)$ and $\bar{\Delta}_i(K)$ for $i = 2 \div 5$ have been found to be negligible. Only the differences between $\Delta_1(K)$ and $\bar{\Delta}_1(K)$ are sizable. In any case the behavior of $\bar{\Delta}_i(K)$ for large K is the same as that discussed for $\Delta(K)$. Therefore, we propose to estimate the “total missing” BE by using the formula

$$(\Delta B)_T = \sum_{i=1,6} c(K_{iM}, p) \bar{\Delta}_i(K_{iM}) ,\tag{4.6}$$

where $p = 5$ (7) for the MT-V potential (AV18 and AV18+UIX). To give an example, the values for $\Delta_i(K_{iM})$ and $c(K_{iM}, p)$ computed for the MT-V case are reported in Table IV, from which it is possible to derive that $(\Delta B)_T \approx 11$ keV. If this value is added to $B(72, 40, 34, 28, 0, 0) = 31.347$ MeV, we obtain 31.358 MeV, which is in very good agreement with the results obtained by other groups. For the AV18 potential, Eq. (4.6) gives $(\Delta B)_T = 12$ keV and if this value is added to $B(72, 40, 34, 28, 24, 16) = 24.210$ MeV, we obtain 24.222 in close agreement with the FY estimates of 24.25 MeV of Ref. [51] and 24.223 of Ref. [54]. Note that for the class C2 we have computed the coefficient $c(\bar{K}, p)$ with $p = 7$. Using $p = 6$, we have $c(40, 6) = 3.52$ and $(\Delta B)_2 = 3.20$ keV (instead of 2.60 keV), a very small change. For the AV18+UIX model, the same procedure allows for an extrapolated BE estimate of 28.474 MeV, again in agreement with the FY value 28.50 MeV. Note that the FY BE results are quoted with an uncertainty of 50 keV due to the truncated model space in their calculations [51].

B. Results

The values obtained for a number of different potential models after including the states of the 6 different classes up to the values $K_1 = 72$, $K_2 = 40$, $K_3 = 34$, $K_4 = 28$, $K_5 = 24$ and $K_6 = 16$ (the last two values only for the realistic cases, for central potential we have taken $K_5 = K_6 = 0$) are presented in Tables V and VI. Table V presents the results for some central potential models, while Table VI reports the results for various realistic potentials with and without including different models for the 3N forces, too. The BE’s obtained by using the extrapolation technique described in the previous section are enclosed in parentheses. Results obtained by other techniques are also reported.

Let us consider first the central potentials (for all of them we have taken $\hbar^2/m = 41.47$ MeV fm²). We have selected 5 different potential models, i.e. the Volkov [55], the Afnan-Tang S3 (ATS3) [56], the Minnesota [57], the MT-V and the Malfliet-Tjon version I/III (MT-I/III) [48]. These potentials have been used by several groups to produce benchmark calculations, but unfortunately for some of them different versions exist. The parameters of the first 4 potentials mentioned above can be found in Table I of Ref. [20], while the version of the MT-I/III used has the same parameters as reported in Table I of Ref. [18]. The Volkov and MT-V are spin-independent, while the other 3 potentials are spin dependent. Note that it is customary to include the point-Coulomb interaction ($e^2 = 1.44$ MeV fm) with the Minnesota potential, while the MT-I/III version acts only on s-waves. Clearly for this group of potentials,

the total orbital angular momentum is a good quantum number and therefore we have included in the WF's only the channels with $L = 0$.

The first example is the Volkov potential with Majorana parameter $M = 0.6$. As can be seen in Table V, our result agrees very well with the estimates by other techniques, especially with the one using the SVM [20]. The Volkov potential, given as a sum of gaussians, has a very soft core and therefore the induced two-body correlations in the ground state WF are weaker than in the other cases. In fact, we have found that the convergence of the HH expansion is in this case much faster (it is reached for $K_1 \approx 30$). Since inclusion of HH states with fairly low values of the grand angular quantum number are sufficient to obtain convergence, a successful HH calculation for this potential was already possible 20 years ago [35].

Others central potentials often used in the literature are the ATS3 and Minnesota potentials. Both are given as a sum of gaussians but have a rather strong repulsion at short interparticle distances. This induces important two-body correlations in the WF's and consequently an acceptable convergence for the first class is reached only for $K_1 > 40$. The chosen version of the Minnesota potential has the exchange parameter $u = 1$. As mentioned before, the point-Coulomb potential is included in the calculation, however, in the WF we have included only states with $T = 0$. In both cases, we observe a good agreement between the different theoretical estimates.

The three potentials examined so far are given as functions of gaussians and thus depend on r_{ij}^2 . As is well known, in such a case the convergence of the HH expansion as a function of the grand angular quantum number is exponential and fast. We actually observe such a behavior in all three cases. However, especially for the class C1, the convergence is relatively more difficult for the two models with a repulsive core than in the Volkov case, confirming that it is this class which is mostly responsible for the need of the two-body correlations.

The next examples considered are the MT-V and MT-I/III potentials. They are given as a superposition of Yukawians and have a strong repulsive core with a $1/r$ divergence. As already mentioned they represent the most challenging problem for the HH expansion, due to the difficulty of constructing accurate two-body correlations at short interparticle distances, where the cancellation between kinetic and potential energy is critical. As can be seen by inspecting Table V, the BE for the MT-V is slightly underestimated. We have already discussed this case in the previous subsection and we have seen that it is possible to obtain very precise estimates for the “missing” BE using the known behavior $\Delta \propto 1/\bar{K}^5$. Adding this “missing” BE to the value $B = 31.347$ MeV brings the HH results very close to the estimates computed by other techniques. For the (s-wave) MT-I/III we observe that our estimate is already close to the very precise calculation of Ref. [18]. The “missing” BE in this case is estimated to be 21 keV, bringing our estimated BE to be 30.331 MeV.

Let us now consider the calculations performed using the realistic models of the NN interactions (see Table VI). Again the value $\hbar^2/m = 41.47108$ MeV fm², corresponding to $2/m = 1/m_p + 1/m_n$, has been used. Let us consider first the calculations performed without any 3N interaction. We have considered here the AV18 and the Nijmegen II [6] (Nijm-II) interactions models. Both potentials belong to the group of the modern NN potentials which reproduce the NN Nijmegen data set [59] with a χ^2 per datum ≈ 1 . They have been selected since they are local in coordinate space, while other modern potentials either have a “non-local” term like ∇^2 (Nijmegen I potential [6]), or are given in momentum space (Bonn interaction [7]). Note that our technique does not, in principle, present any difficulties in treating these other kind of potentials. The only problem is that now it is not possible to solve the hyperradial second order differential equations by the method proposed in Ref. [46]. Work is in progress to overcome this difficulty and to compute the $A = 3$ and 4 WF's also with non-local potentials in coordinate or momentum space.

The convergence of the HH expansion in the case of the AV18 potential has been already discussed in the previous subsection. An analogous pattern of convergence is also found for the Nijm-II potential. In Table VI, the results for the BE and other properties are compared with the results of other techniques. Note that in the Nijm-II model we have included also the electro-magnetic interactions, in addition to the Coulomb potential, as in the case of the AV18 potential. These terms contribute an additional -0.07 MeV to the BE and this explains the difference with the reported FY calculation, where they were not included. By taking into account this fact, our Nijm-II BE agrees well with the corresponding value obtained using the FY equations. Moreover, by taking into account the “missing” BE estimated as explained previously, our results practically reproduce the FY ones, by again taking into account the quoted 50 keV uncertainty of the latter method [51].

We now consider the inclusion of the 3N interaction. We have considered here two models: the already discussed UIX and Tucson-Melbourne [11] (TM) model. In the latter case, we have used the modified version TM', more consistent with chiral symmetry [60], with the cutoff parameter fixed to be $\Lambda = 4.756 m_\pi$ [3]. We have used them together with the AV18 potential (AV18+UIX and AV18+TM' models). The cutoff parameter of the TM' 3N interaction was chosen to reproduce the BE of ^3He . The inclusion of the UIX or the TM' models of the 3N interaction does not change the convergence behavior of the HH expansion and also in these cases it is possible to obtain nearly converged results (they have been obtained in the approximation described in Subsec. IVD). Note that in the AV18+UIX case, the HH and FY estimates for the BE are slightly above the GFMC result. This is probably due to fact that in the GFMC technique, the L^2 and $(L \cdot S)^2$ terms of the NN interaction are not treated exactly and therefore the GFMC

estimates have to be regarded as an upper bound of the true ground state energy.

In summary, the HH expansion has proved to be flexible enough to describe accurately the α -particle bound state using realistic NN and 3N interaction models.

C. Origin of the $T > 0$ components

In the calculations performed with the realistic NN and NN+3N interaction we have included components with total isospin $T = 0, 1$ and 2 in the WF. The calculated percentages of the waves with $T = 1$ and $T = 2$ for the AV18 and AV18+UIX models are reported in Table VII. The results obtained by the FY calculations [51] have been also reported. These components appear in the WF when the class C6 is included in the expansion. From Table III, it can be seen that the convergence of the BE for that class is reached without difficulties including states up to $K = 16$. However, the percentage values of the $T = 1$ and 2 states have been found to converge substantially more slowly and HH functions of class C6 up to $K = 32$ have to be considered. The contribution to the BE of the C6 states with $K > 16$ is very small, less than 1 keV.

As can be seen by inspecting Table VII, the percentages of the components with $T = 1$ and $T = 2$ in the α -particle wave function are extremely small. For the AV18 potential, they are in good agreement with the FY estimates [51]. The percentages obtained using the Nijm-II potential differ by about 40% with respect to those obtained with the AV18. The inclusion of the 3N interaction tends to reduce them slightly. The adopted models of 3N interaction do not contain any isospin mixing term.

The knowledge of the $T = 1$ and 2 percentages is important for parity violating experiments of electron scattering on ^4He , devoted to studying the admixture of strange quark $s\bar{s}$ pairs in the nucleon. Information on this quantity can be extracted from the measurement of the “left-right” asymmetry A_{LR} of polarized electrons on a target nucleus, resulting from the interference between the electromagnetic and the weak neutral current mediating the scattering process. The study of the asymmetry is particularly simple in case of a $(J^\pi, T) = (0^+, 0)$ system, since in that case the number of matrix elements entering this observable is small. Moreover, the use of ^4He as a target nucleus is also favored by the fact that its first excited state is at 20.1 MeV, which allows for an easy experimental control of inelastic processes. Indeed, there are approved experiments at the Jefferson Lab [61, 62].

However, the extraction of the information from the experiments could be complicated by the presence of components with isospin $T = 1$ and 2 in the WF of ^4He . This question was analyzed in Ref. [63] and found that the contribution from the $T = 1$ isospin mixing configurations to A_{LR} was negligible. Considering the effect of the Coulomb potential alone, the percentage of the $T = 1$ component in that work was estimated to be $P_{T=1} = 7 \times 10^{-4}$. From the present calculation, in agreement with the study of Ref. [51], the $T = 1$ component results to be 4 times larger and this could be of some effect on A_{LR} .

It is interesting to study the origin of the $T = 1$ and 2 isospin admixtures to the α particle WF. To this end we have performed a series of calculations by removing from the Hamiltonian the different terms which induce the $T > 0$ components. Let us write

$$H = H_{IC} + H_C + H_{CSB} + H_{e.m.} + K_\Delta, \quad (4.7)$$

where H_{IC} is the isospin-conserving part of the nuclear Hamiltonian, H_C the point-Coulomb interaction, H_{CSB} the charge symmetry breaking nuclear interaction (namely, the operators 15-18 in AV18), $H_{e.m.}$ the remaining electro-magnetic (e.m.) interaction (finite-size effects, vacuum polarization, magnetic moment interactions, etc) and K_Δ the term originating from the proton and neutron mass difference in the kinetic energy. This latter term has not been included in the solution of the four body problem and its effects have been evaluated perturbatively as explained below.

By approximating the Hamiltonian with H_{IC} only, one would get no isospin admixture at all. We have then added the various terms one by one to H_{IC} , and reported the results in Table VIII. As can be seen from that table, with the inclusion of the Coulomb potential H_C , the percentage of the $T = 1$ state is in rough agreement (within a factor 2) with that estimated in Ref. [63]. The percentage of the $T = 2$ state is very tiny in this case. When the CSB terms of the AV18 NN interaction are taken into account, however, the previous picture is noticeably modified and both components increase, in particular the $T = 2$ component which becomes larger than the $T = 1$ one. Finally, the effect of $H_{e.m.}$ is rather tiny.

To further analyze the origin of the isospin admixture components, we have repeated the approximate calculation of Ref. [63]. Let us write

$$H_C + H_{CSB} + H_{e.m.} + K_\Delta \equiv H_I^{(0)} + H_I^{(1)} + H_I^{(2)}, \quad (4.8)$$

namely as a sum of an isoscalar, isovector and isotensor term (the isoscalar part comes from the Coulomb and e.m. potentials). Let us treat $H_{IC} + H_I^{(0)}$ as the unperturbed Hamiltonian, and try to evaluate the $T > 0$ components using first order perturbation theory. Namely,

$$|\delta\Psi^{(T)}\rangle = \sum_{n>0} |\Psi_n\rangle \frac{\langle\Psi_n|H_I^{(T)}|\Psi_0\rangle}{E_0 - E_n}, \quad (4.9)$$

where Ψ_0 is the unperturbed ground state and Ψ_n , $n = 1, 2, \dots$ the unperturbed excited states of $H_{IC} + H_I^{(0)}$, which therefore have definite values of the total isospin quantum number. In particular, Ψ_0 has $T = 0$, etc. The most important contributions to the components $T = 1, 2$ of $\delta\Psi^{(T)}$ would come from the lowest excited states. Following Ref. [63] (see also Ref. [64]), we model these states as

$$|\Psi_1^{(T)}\rangle = \frac{\Omega_T|\Psi_0\rangle}{\langle\Psi_0|\Omega_T^\dagger\Omega_T|\Psi_0\rangle^{1/2}}, \quad (4.10)$$

where Ω_T , $T = 1, 2$, are excitation operators of the form

$$\Omega_1 = \sum_{ij} r_{ij}^2 (\tau_z(i) + \tau_z(j)), \quad (4.11)$$

$$\Omega_2 = \sum_{ij} r_{ij}^2 (\tau_z(i)\tau_z(j) - (1/3)\boldsymbol{\tau}(i) \cdot \boldsymbol{\tau}(j)). \quad (4.12)$$

The operator Ω_1 generates a state $(J^\pi, T) = (0^+, 1)$ corresponding to a “breathing” mode where neutrons and protons oscillate in counter-phase. Furthermore, Ω_2 generates a state $(J^\pi, T) = (0^+, 2)$ with “tensor” oscillations. The $T = 1, 2$ components in the ${}^4\text{He}$ wave function would be given by

$$|\delta\Psi^{(T)}\rangle \approx |\Psi_1^{(T)}\rangle \frac{\langle\Psi_1^{(T)}|H_I^{(T)}|\Psi_0\rangle}{E_0 - E_1(T)} \equiv \chi_T |\Psi_1^{(T)}\rangle, \quad (4.13)$$

where $E_1^{(T)} = \langle\Psi_1^{(T)}|H_{IC} + H_I^{(0)}|\Psi_1^{(T)}\rangle$. The percentage of the T -wave is just $100|\chi_T|^2$.

In the following, we applied the procedure outlined above using the AV18 potential model. Ψ_0 is the WF computed with the HH expansion excluding any states belonging to the class C6. We have found

$$E_0 = -24.19 \text{ MeV}, \quad E_1^{(1)} = 7.05 \text{ MeV}, \quad E_1^{(2)} = 29.07 \text{ MeV}. \quad (4.14)$$

Let us first consider the (point) Coulomb potential H_C , given by

$$H_C = \sum_{i<j} \frac{e^2}{r_{ij}} \left(\frac{1 + \tau_z(i)}{2} \right) \left(\frac{1 + \tau_z(j)}{2} \right) \quad (4.15)$$

and therefore

$$H_{I,C}^{(1)} = \sum_{i<j} \frac{e^2}{r_{ij}} \left(\frac{\tau_z(i) + \tau_z(j)}{4} \right), \quad (4.16)$$

$$H_{I,C}^{(2)} = \sum_{i<j} \frac{e^2}{r_{ij}} \left(\frac{\tau_z(i)\tau_z(j) - \frac{1}{3}\boldsymbol{\tau}(i) \cdot \boldsymbol{\tau}(j)}{4} \right). \quad (4.17)$$

The necessary matrix elements can be readily computed with the result that

$$\langle\Psi_1^{(T=1)}|H_{I,C}^{(T=1)}|\Psi_0\rangle \approx -100 \text{ keV}, \quad \langle\Psi_1^{(T=2)}|H_{I,C}^{(T=2)}|\Psi_0\rangle \approx -37 \text{ keV}. \quad (4.18)$$

and therefore $P_{T=1} \approx 1 \times 10^{-3}$ and $P_{T=2} \approx 0.05 \times 10^{-3}$ confirming that the $T = 2$ component induced by the Coulomb potential is smaller than the $T = 1$ one. In fact, the radial dependence (and strength) of $H_{I,C}^{(1)}$ and $H_{I,C}^{(2)}$ are the same. However, the $T = 2$ breathing mode has a higher excited energy and this reduces the probability of a “transition” to the state $|\Psi_1^{(T=2)}\rangle$. The values $P_{T=1}$ and $P_{T=2}$ are also in rough agreement (within a factor 2) with the results reported in the second row of Table VIII. It appears that in our approximate calculation, the $T = 1$ and

2 percentages are somewhat underestimated. Note that the value $P_{T=1} \approx 1 \times 10^{-3}$ is also in reasonable agreement with the estimate of Ref. [63].

As seen before, this situation is reversed when the CSB part of the nuclear interaction is taken into account. The CSB part of the AV18 potential is explicitly given by

$$H_{CSB} = \sum_{i < j} \left(V^{(1)}(i, j) [\tau_z(i) + \tau_z(j)] + V^{(2)}(i, j) [\tau_z(i) \tau_z(j) - \frac{1}{3} \boldsymbol{\tau}(i) \cdot \boldsymbol{\tau}(j)] \right) \equiv H_{I,CSB}^{(1)} + H_{I,CSB}^{(2)}, \quad (4.19)$$

where $V^{(1)}(i, j)$ and $V^{(2)}(i, j)$ are functions depending on the interparticle distance r_{ij} and on the spin operators of the particles i and j . The operator $[\tau_z(i) \tau_z(j) - \frac{1}{3} \boldsymbol{\tau}_i \cdot \boldsymbol{\tau}_j]$ in $H_{I,CSB}^{(2)}$ induces differences between the pp and pn interactions (it originates mainly from the difference between the charged and neutral pion masses). These differences are well established and, although rather small, are of sizable value in some observables (such as the singlet np and pp scattering lengths). The operator $[\tau_z(i) + \tau_z(j)]$ in $H_{I,CSB}^{(1)}$ induces instead differences between the pp and nn interaction, too. Due to the lack of precise nn data, the magnitude of this charge independence breaking term is not very well known, however, its strength should satisfy $H_{CSB}^{(1)} \ll H_{CSB}^{(2)}$. Turning to our approximate method, we have found that

$$\langle \Psi_1^{(T=1)} | H_{I,CSB}^{(T=1)} | \Psi_0 \rangle \approx -23 \text{ keV}, \quad \langle \Psi_1^{(T=2)} | H_{I,CSB}^{(T=2)} | \Psi_0 \rangle \approx -84 \text{ keV}. \quad (4.20)$$

As expected, the matrix elements $\langle \Psi_1^{(T=2)} | H_{I,CSB}^{(T=2)} | \Psi_0 \rangle$ are larger than the corresponding matrix elements of $H_{I,CSB}^{(1)}$. Adding the values given in Eqs. (4.18) and (4.20), we find $P_{T=1} = 1.5 \times 10^{-3}$ and $P_{T=2} = 0.6 \times 10^{-3}$ as the percentage of the isospin components induced by the Coulomb+CSB part of the Hamiltonian. Our approximate calculation seems to underestimate both component percentages (in particular $P_{T=2}$), but it is in qualitative agreement with the results reported in Table VIII.

The e.m. part of the Hamiltonian produces small effects. This is also supported by our approximate calculation. We have found, in fact, that

$$\langle \Psi_1^{(T=1)} | H_{\text{e.m.}} | \Psi_0 \rangle \approx 6 \text{ keV}, \quad \langle \Psi_1^{(T=2)} | H_{\text{e.m.}} | \Psi_0 \rangle \approx -3 \text{ keV}. \quad (4.21)$$

The last effect which should be taken into consideration is the mass difference between neutrons and protons. The associated term in the Hamiltonian is

$$H_\Delta = \sum_{i=1,4} \frac{1}{2} \left(\frac{1}{2m_p} - \frac{1}{2m_n} \right) \nabla_i^2 \tau_z(i) \equiv H_{I,\Delta}^{(1)}, \quad (4.22)$$

and therefore H_Δ is an isovector operator and may increase the percentage of the $T = 1$ state. We have not considered this term in the solution of the full four-body problem but we have estimated its contribution using the approximated procedure outlined before. We have found that

$$\langle \Psi_1^{(T=1)} | H_{I,\Delta}^{(T=1)} | \Psi_0 \rangle \approx -9 \text{ keV}. \quad (4.23)$$

The effect of H_Δ is therefore rather small (it would produce a change of $P_{T=1}$ of about 0.1×10^{-4}).

This study therefore roughly support the result of our full calculation, namely that the charge symmetry breaking terms of the nuclear interaction are responsible for the relatively large $T = 2$ components in the α -particle wave function. On the contrary, the $T = 1$ component originates mainly from the Coulomb interaction. The other e.m. terms and the neutron-proton mass difference play a negligible role.

D. Truncation studies

In prevision of future applications of the present technique to heavier systems, we have explored the effect of truncating part of the NN and 3N interaction. The aim is to find a way of simplifying the Hamiltonian, still obtaining very precise results, with a maximum deviation of the order of 0.1% with respect to the results obtained without any approximation. We have explored both the effect of neglecting the NN interaction when the total angular momentum j of the pair is greater than a given value j_M and the effect of neglecting the 3N interaction when it acts on HH states with grand angular quantum number greater than a given K_M .

Let us first discuss the case of truncation of the NN interaction. We have considered an NN interaction which vanishes when acting on pairs with total angular momentum $j > j_M$, and have varied j_M to see the effect on the

α -particle BE. We have considered the AV18 interaction, since its operatorial form allows one to compute it for arbitrary values of j . The results obtained can be seen in Table IX. The calculation with $j_M = \infty$ means that we have retained the NN interaction acting in all states. By inspecting the Table, it can be seen that by taking $j_M \geq 6$ the BE and other quantities vary very little. Therefore, it seems safe to retain the NN interaction as acting only on states with $j \leq 6 \div 8$.

Let us now consider the 3N interaction. The behavior of the radial parts of the UIX or TM' 3N potential are rather soft at short interparticle distances. Since the large grand angular quantum number components in the WF are induced by the repulsive core of the potentials, this suggests that the correlations induced by the 3N interaction would not need such high components. Therefore, we have included in the Hamiltonian an effective 3N interaction of the kind

$$\widetilde{W}_{K_M}(i, j, k) = P_{K_M}^\dagger W(i, j, k) P_{K_M} \quad (4.24)$$

where $W(i, j, k)$ is one of the standard 3N interactions and P_{K_M} a projection operator which gives 0 when it acts on four body HH states with a given grand angular quantum number K if $K > K_M$. Actually, $\widetilde{W}_{K_M}(i, j, k)$ is an effective 4-body interaction. We have then studied the effects on the α -particle BE by varying K_M . We have considered here the AV18+UIX model. The results obtained can be found in Table X, where for simplicity we have restricted the HH basis to include only the first three classes (in any case, the other classes include HH states with $K < 30$). As can be seen by inspecting the Table, the BE and the other quantities depend very little on K_M . Already for $K_M = 20$, the corresponding BE differs from that obtained in the non-truncated case by less than 0.1%. The calculation of the 3N potential matrix elements between states with $K \leq 20 \div 30$ is noticeably simpler than in the general case and still the results are of acceptable precision. This should allow for HH calculations including 3N interactions also for scattering states and for heavier systems. This conclusion is also supported by the study of Ref. [65] of the incorporation of the 3N interaction in the EIIH method. Note that the results reported in Tables III and VI have been obtained using the 3N interactions “truncated” as in Eq. (4.24) and taking $K_M = 30$.

E. Asymptotic Normalization Constants

The asymptotic normalization constants (ANC's) are properties of the bound state WF which can be related to experimental observables. They are interesting quantities from which useful information on the nuclear structure can be extracted. They also provide a test of the quality of the variational WF in the asymptotic region, as we shall see. This test will be particularly severe in our approach, as the description of the ^4He WF in terms of the four-body HH functions in regions where the 1+3 or 2+2 clustering configurations are dominant will be difficult.

Let us concentrate first on the proton-triton ANC C_S^{pt} of ^4He , defined by

$$\Psi_4(\xi_1, \xi_2, \xi_3) \rightarrow C_S^{pt} \sqrt{2\beta_{pt}} \frac{W_{-\eta_{pt}, 1/2}(2\beta_{pt} r_{pt})}{r_{pt}} \Phi_0^{pt}(\widehat{\xi}_1, \xi_2, \xi_3), \quad r_{pt} \rightarrow \infty, \quad (4.25)$$

where the Jacobi vectors ξ_i correspond to the permutation $p = 1$ (the index p will be suppressed in this section) and $r_{pt} = \sqrt{2/3} \xi_1$ is the distance between the ^3H center of mass and the fourth nucleon. The function Φ_L^{pt} is defined as

$$\Phi_L^{pt}(\widehat{\xi}_1, \xi_2, \xi_3) = \left\{ Y_L(\widehat{\xi}_1) \left[\psi_t(1, 2, 3) \chi_4 \xi_4 \right]_S \right\}_{0,0}, \quad (4.26)$$

where $\psi_t(1, 2, 3) \equiv \psi_t(\xi_2, \xi_3)$ is the ^3H WF and $\chi_4(\xi_4)$ is the spin (isospin) function of the fourth nucleon. In the previous equation, the spin 1/2 of ^3H is coupled to the spin 1/2 of the other nucleon to give a “channel” spin $S = 0, 1$. The channel spin is in turn coupled to L to give a total angular momentum $J = 0$, therefore $L = S$. Due to the even parity of the ^4He state, the $p - ^3\text{H}$ clusters can only be in the state $S = L = 0$. In Eq. (4.25), $W_{-\eta, j}(2\beta r)$ is the Whittaker function which behaves irregularly at the origin and decays exponentially for $r \rightarrow \infty$, while β_{pt} and η_{pt} are determined by

$$\beta_{pt} = \sqrt{\frac{3}{2} \frac{m}{\hbar^2} (B_4 - B_t)}, \quad \eta_{pt} = \frac{3}{4} \frac{m}{\hbar^2} \frac{e^2}{\beta_{pt}}, \quad (4.27)$$

where $e^2 \approx 1.44 \text{ MeV fm}$, $\hbar^2/m \approx 41.47 \text{ MeV fm}^2$ and B_4 and B_t are the ^4He and ^3H BE, respectively. Finally, the factor $\sqrt{2\beta_{pt}}$ in Eq. (4.25) has been introduced so that the ANC C_S^{pt} be adimensional.

In order to calculate C_S^{pt} , let us introduce the ${}^3\text{H} - {}^4\text{He}$ overlap function as

$$f_{pt}(r_{pt}) = \int d^3\xi_1 d^3\xi_2 d^3\xi_3 \delta\left(\sqrt{\frac{2}{3}}\xi_1 - r_{pt}\right) \frac{\Phi_0^{pt}(\hat{\xi}_1, \xi_2, \xi_3)^\dagger}{r_{pt}} \Psi_4(\xi_1, \xi_2, \xi_3), \quad (4.28)$$

and the ratio

$$c_{pt}(r_{pt}) = \frac{f_{pt}(r_{pt})}{(3/2)^{\frac{3}{2}} \sqrt{2\beta_{pt}} W_{-\eta_{pt}, 1/2}(2\beta_{pt}r_{pt})}. \quad (4.29)$$

If Ψ_4 is the exact ${}^4\text{He}$ WF, for $r_{pt} \rightarrow \infty$ the overlap function behaves as

$$f_{pt}(r_{pt}) \rightarrow \left(\frac{3}{2}\right)^{\frac{3}{2}} C_S^{pt} \sqrt{2\beta_{pt}} W_{-\eta_{pt}, 1/2}(2\beta_{pt}r_{pt}), \quad (4.30)$$

and therefore $c_{pt}(r_{pt}) \rightarrow C_S^{pt}$, allowing for the extraction of the ANC. The ${}^3\text{H}$ WF has been determined by means of the pair-correlated HH (PHH) technique described in Ref. [27] and is believed to be very precise [66]. The dependence to the truncation level of the HH basis used to compute the ${}^4\text{He}$ WF has been studied by computing the overlap function for the following three different choices of the maximum values of the grand angular quantum numbers of the six classes as defined in Subsec. IV A,

$$\begin{aligned} \{K_{1M}, K_{2M}, K_{3M}, K_{4M}, K_{5M}, K_{6M}\} &= \{56, 32, 26, 16, 14, 24\}, & \text{case a}, \\ \{K_{1M}, K_{2M}, K_{3M}, K_{4M}, K_{5M}, K_{6M}\} &= \{60, 36, 30, 20, 18, 28\}, & \text{case b}, \\ \{K_{1M}, K_{2M}, K_{3M}, K_{4M}, K_{5M}, K_{6M}\} &= \{64, 40, 34, 24, 22, 32\}, & \text{case c}. \end{aligned} \quad (4.31)$$

The corresponding ratios c_{pt} are shown in Fig. 3 by the open circles (case a), open squares (case b) and solid triangles (case c). The potential used to generate the WF is the AV18 interaction. As can be seen by inspection of the figure, all three functions c_{pt} start to deviate from the expected asymptotic constant behavior already for $r_{pt} > 5$ fm, showing the difficulty of reproducing the cluster structure of the WF by means of the four-body HH functions. From the differences between the three ratios, the very slow convergence of $c_{pt}(r)$ as a function of $\{K_{1M}, K_{2M}, K_{3M}, K_{4M}, K_{5M}, K_{6M}\}$ results to be evident. In particular, a detailed analysis has shown that the convergence is sensitive to the value of K_{1M} . The ratio $c_{pt}(r)$ obtained with the larger basis shows a slightly larger “plateau” around $r_{pt} = 5$ fm, allowing for a crude estimate of the ANC, $C_S^{pt} \approx 1.7$.

To obtain a greater accuracy in the extraction of the ANC we have followed another procedure [67]. Assuming that Ψ_4 and ψ_t are “exact”, it is not difficult to show that the overlap function should satisfy the following differential equation

$$-\frac{2}{3} \frac{\hbar^2}{m} f_{pt}''(r) + \frac{e^2}{r} f_{pt}(r) + (B_4 - B_t) f_{pt}(r) + g(r) = 0, \quad (4.32)$$

where $r \equiv r_{pt}$ and

$$\begin{aligned} g(r) = \int d^3\xi_1 d^3\xi_2 d^3\xi_3 \delta\left(\sqrt{\frac{2}{3}}\xi_1 - r\right) \frac{\Phi_0^{pt}(\hat{\xi}_1, \xi_2, \xi_3)^\dagger}{r_{pt}} &\left[V_{14} + V_{24} + V_{34} \right. \\ &\left. + W_{124} + W_{134} + W_{234} - \frac{e^2}{r} \right] \Psi_4(\xi_1, \xi_2, \xi_3), \end{aligned} \quad (4.33)$$

V_{ij} and W_{ijk} being the NN and 3N potential, respectively. As $r \rightarrow \infty$, the function $g(r) \rightarrow 0$, and the solution of Eq. (4.32) coincides with the Whittaker function, allowing for the extraction of the ANC via Eq. (4.29). We have computed the function $g(r)$ with the three different choices of the ${}^4\text{He}$ WF Ψ_4 given in Eq. (4.31) and reported the results in Fig. 4. As can be seen, the function $g(r)$ is peaked at $r \approx 2$ fm, goes to zero exponentially and depends slightly on the choice of Ψ_4 . In fact, the selected HH bases are already large enough to accurately describe the $p - {}^3\text{H}$ decomposition for $r < 4$ fm. For larger distances, probably $g(r)$ is not computed accurately using our variational WF, but there $g(r)$ becomes vanishingly small and the resulting effect on the ANC is negligible. This has been checked explicitly by solving Eq. (4.32) (imposing the boundary conditions $f_{pt}(0) = f_{pt}(\infty) = 0$) and computing $c_{pt}(r)$ for the same three cases as before. The results for $c_{pt}(r)$ are shown in Fig. 3 by the dotted, dashed and solid lines (the results of the latter two cases are practically indistinguishable). As expected, for $r < 5$ fm, the line goes through the ratio functions $c_{pt}(r)$ computed directly via the overlap integral and reaches a constant value, corresponding to

C_S^{pt} , around $r = 5$ fm. The extraction of the ANC can be now achieved without any difficulty and the value found is $C_S^{pt} = 1.715$.

An analogous procedure have been repeated for the $n - {}^3\text{He}$ ANC and the S- and D-wave $d - d$ ANC's. We have used the definition

$$\Psi_4 \rightarrow C_S^{nh} \sqrt{2\beta_{nh}} \frac{e^{-\beta_{nh}r_{nh}}}{r_{nh}} \Phi_0^{nh}(\hat{\xi}_1, \xi_2, \xi_3), \quad r_{nh} = \sqrt{\frac{2}{3}}\xi_1 \rightarrow \infty, \quad (4.34)$$

$$\Psi_4 \rightarrow C_S^{dd} \sqrt{2\beta_{dd}} \frac{W_{-\eta_{dd}, 1/2}(2\beta_{dd}r_{dd})}{r_{dd}} \Phi_0^{dd}(\xi'_1, \hat{\xi}'_2, \xi'_3) \quad (4.35)$$

$$+ C_D^{dd} \sqrt{2\beta_{dd}} \frac{W_{-\eta_{dd}, 5/2}(2\beta_{dd}r_{dd})}{r_{dd}} \Phi_2^{dd}(\xi'_1, \hat{\xi}'_2, \xi'_3), \quad r_{dd} = \sqrt{\frac{1}{2}}\xi'_2 \rightarrow \infty, \quad (4.36)$$

where ξ'_i are the set B of the Jacobi vectors defined in Eq. (3.1) corresponding to the permutation $p = 1$ and

$$\Phi_L^{nh}(\hat{\xi}_1, \xi_2, \xi_3) = \left\{ Y_L(\hat{\xi}_1) \left[\psi_h(1, 2, 3) \chi_4 \xi_4 \right]_S \right\}_{0,0}, \quad (4.37)$$

$$\Phi_L^{dd}(\xi'_1, \hat{\xi}'_2, \xi'_3) = \left\{ Y_L(\hat{\xi}'_2) \left[\phi_d(1, 2) \phi_d(3, 4) \right]_S \right\}_{0,0}. \quad (4.38)$$

In the latter, ψ_h and ϕ_d are the ${}^3\text{He}$ and deuteron WF, respectively, and

$$\beta_{nh} = \sqrt{\frac{3}{2} \frac{m}{\hbar^2} (B_4 - B_h)}, \quad \beta_{dd} = \sqrt{\frac{2m}{\hbar^2} (B_4 - 2B_d)}, \quad \eta_{dd} = \frac{m}{\hbar^2} \frac{e^2}{\beta_{dd}}, \quad (4.39)$$

with B_h and B_d the ${}^3\text{He}$ and deuteron BE, respectively. For the $d - d$ case, one can also estimate the distorted-wave parameter D_2 defined by

$$D_2 = \frac{1}{15} \int_0^\infty dr_{dd} r_{dd}^3 f_{dd}^D(r_{dd}) / \int_0^\infty dr_{dd} r_{dd} f_{dd}^S(r_{dd}), \quad (4.40)$$

where $f_{dd}^X(r_{dd})$ ($X = S, D$) are the S- and D-wave $(d - d) - {}^4\text{He}$ overlap functions, respectively, defined in analogy to Eq. (4.28). The results obtained have been reported in Table XI, together with some other theoretical and experimental estimates available for D_2 (for a more complete list of references, see Ref. [68]). The D_2^{dd} parameter was determined in Ref. [68] using an approximated method (a cluster model) which however seems to provide an estimate rather close to ours. This parameter is also in reasonable agreement with the experimental values reported in Table XI, also considering the difficulty of the extraction of this quantity from the experimental data.

V. CONCLUSIONS AND PERSPECTIVES

We have studied the solution of the Schroedinger equation for the four-nucleon ground state using the HH function expansion. The main difficulty when using the HH basis is its large degeneracy, accordingly a suitable selection of the HH functions giving the most important contributions has to be performed. In this work, the HH functions have been divided into classes, depending on the number of correlated particles, the values of the orbital angular momenta, the total isospin quantum number, etc. For each class, the expansion has been truncated so as to obtain the required accuracy. We have applied this procedure in particular to the study of the ground state of the α -particle using a number of NN and NN+3N interaction models. In all the cases, accurate calculations of the BE and other ground state properties, such as the asymptotic normalization constants, have been achieved.

A similar procedure can be also applied for solving scattering problems. The calculation of the phase shifts and the various observables for $n - {}^3\text{H}$ and $p - {}^3\text{He}$ elastic scattering is now in progress and will be published elsewhere [72].

The hyperspherical formalism is adequate for treating all kinds of modern potentials, except those containing a hard-core. We have considered here the AV18 and Nijmegen-II NN potentials and the UIX and TM' 3N interactions. The inclusion of the ∇^2 term present in the Nijmegen-I [6] potential does not introduce additional difficulties. As an example, such a term was taken into account in ref. [73] where the PHH approach was used. Moreover, the HH method can be easily formulated in momentum space. It can therefore be applied also to the case of the Bonn potential [7] although one additional numerical integration and the solution of an integral equation are then required. The application of the HH technique to the $A = 3, 4$ systems with the Bonn potential is actually under way.

At present there are only a few other methods available for accurate calculations of the four-nucleon problem, in particular by taking into account a 3N force. There are two other important motivations behind this work. The first one is to show in details that the HH expansion applied to the four-nucleon bound and scattering problems is very powerful even for realistic NN interactions. The second motivation is the possibility of the extension of the method to larger systems. The feasibility of such an application would require the solution of the following different problems. First, the calculation of the generalized “Raynal-Revai” coefficients, namely, of the coefficients relating HH functions constructed with different sets of Jacobi vectors. The direct generalization of the algorithm proposed in Ref. [45] is adequate for $A = 5 \div 8$. Otherwise, different algorithms could be used [42, 43, 44]. Second, the computation of the matrix elements of NN and 3N interactions, which can be reduced to the evaluation of low-dimensional integrals as in the present case. In particular, the possibility of approximating the 3N interaction as acting only on HH functions of low K , as discussed in Sec. IV D, should appreciably simplify this task. Finally, the choice of an optimal subset of HH functions. As A grows, the number of HH states for a given K increases very rapidly. The criteria for selecting the subclasses of HH functions chosen in the present paper can be readily generalized to systems with $A > 4$. However, additional properties of the HH function could be exploited to further reduce the number of terms in the expansion. For example, one could take into account the symmetry of the space part of the states constructed as a product of the HH functions and the spin-isospin states. Another possibility to be explored is to include classes of HH functions constructed with those Jacobi vectors pertaining to different partitions of the particles. For example, in the study of the $d + {}^3\text{H} \rightarrow {}^4\text{He} + p$ reaction, the use of HH functions constructed in terms of $2 + 3$ and $4 + 1$ clusterizations should be very useful.

VI. ACKNOWLEDGMENTS.

The author would like to thank Prof. R. Schiavilla and Prof. L. Lovitch for useful discussions and a critical reading of the manuscript.

APPENDIX

In this Appendix, the method used for calculating the matrix elements of a local 3N interaction operator H_{3N} between the antisymmetric hyperangular–spin–isospin states defined in Eq. (2.10) will be briefly illustrated. The major problem to be overcome is to achieve a sufficient numerical precision, so that the differential equations for the functions $u_{KLS\mu}(\rho)$ defined in Eq. (2.21) could be solved without any numerical trouble. In general, a 3N interaction is written as follows

$$H_{3N} = \sum_{i < j < k} \sum_{cyclic} W_{3N}(i; j, k) , \quad (1)$$

where \sum_{cyclic} represents a cyclic sum over induces i, j and k and $W_{3N}(i; j, k)$ is symmetric under the exchange of the particles j and k . Therefore, the problem can be reduced to the computation of the matrix element of the operator $W_{3N}(1; 2, 3)$. Once the antisymmetric hyperangular–spin–isospin states are expanded in terms of the jj states as in Eq. (2.22), one has to compute the following integrals:

$$\mathcal{W}_{\nu, \nu'}(\rho) = \int d\Omega \langle \Xi_{\nu}^{KTJ\pi}(1, 2, 3, 4) | W_{3N}(1; 2, 3) | \Xi_{\nu'}^{K'TJ\pi}(1, 2, 3, 4) \rangle , \quad (2)$$

where the states $\Xi_{\nu}^{KTJ\pi}(1, 2, 3, 4)$ are defined in Eq. (2.23) (hereafter all the Jacobi vectors are chosen to correspond to the permutation $p = 1$, and therefore the index p will be omitted). In the case of the Urbana or TM-like 3N interactions, $W_{3N}(1; 2, 3)$ can be taken to have the general form [74]

$$W_{3N}(1; 2, 3) = \sum_{p, q=1}^6 F_{p, q}(r_{12}, r_{13}, \mu_{12, 13}) \mathcal{O}_{12}^p \mathcal{O}_{13}^q , \quad (3)$$

where $\mu_{12, 13} = \hat{\mathbf{r}}_{12} \cdot \hat{\mathbf{r}}_{13}$ and \mathbf{r}_{ij} is the relative distance between the particles i and j . In the latter equation, $\mathcal{O}_{ij}^{p=1, 6}$ are the operators

$$\mathcal{O}_{ij}^{p=1, 6} = 1, (\boldsymbol{\tau}_i \cdot \boldsymbol{\tau}_j), (\boldsymbol{\sigma}_i \cdot \boldsymbol{\sigma}_j), (\boldsymbol{\sigma}_i \cdot \boldsymbol{\sigma}_j)(\boldsymbol{\tau}_i \cdot \boldsymbol{\tau}_j), r_{ij}^2 S_{ij}, r_{ij}^2 S_{ij}(\boldsymbol{\tau}_i \cdot \boldsymbol{\tau}_j) , \quad (4)$$

where S_{ij} is the tensor operator (the factor r_{ij}^2 has been included in the definition of $\mathcal{O}^{p=5, 6}$ so that these operators are polynomials in the Cartesian coordinates of the particles).

Since $W_{3N}(1; 2, 3)$ depends only on the variables $\rho, \varphi_3, \varphi_2, \hat{\xi}_2, \hat{\xi}_3$ we can easily integrate over the variables $\hat{\xi}_1$. Moreover, by evaluating the spin-isospin traces and the integrals over the angles $\hat{\xi}_2, \hat{\xi}_3$ (except for $\mu = \hat{\xi}_2 \cdot \hat{\xi}_3$) one reduces the matrix element given in Eq. (2), to an integral of the type:

$$\mathcal{W}_{\nu, \nu'}(\rho) = \sum_{p, q} \int_{-1}^1 dz \sqrt{1+z} \int_{-1}^1 dx \sqrt{1-x^2} \int_{-1}^1 d\mu F_{p, q}(r_{12}, r_{13}, \mu_{12, 13}) \mathcal{P}_{p, q}(z, x, \mu) \quad (5)$$

where

$$z = \cos 2\varphi_3 = 2 \frac{r_{12}^2}{\rho^2} - 1, \quad x = \cos 2\varphi_2 = 2 \frac{\xi_2^2}{\rho^2} - 1, \quad (6)$$

and

$$\mathcal{P}_{p, q}(z, x, \mu) = \frac{(4\pi)^2}{128\sqrt{2}} \int d\hat{\xi}_1 \langle \Xi_{\nu}^{KTJ\pi}(1, 2, 3, 4) | \mathcal{O}_{12}^p \mathcal{O}_{13}^q | \Xi_{\nu'}^{K'TJ\pi}(1, 2, 3, 4) \rangle. \quad (7)$$

In Eq. (7) the integration over the angles $\hat{\xi}_2, \hat{\xi}_3$ (except for $\mu = \hat{\xi}_2 \cdot \hat{\xi}_3$) and the trace over the spin-isospin degrees of freedom is implicit. This latter part of the calculation can be performed analytically in terms of Wigner D -matrices and Clebsh-Gordan coefficients. The remaining two-dimensional integration over $d\hat{\xi}_1 = d\cos\theta_1 d\phi_1$ in Eq. (7) can be easily performed by taking into account that the integrand is a polynomial in $\cos\theta_1$ and $\cos\phi_1$ of degree $K + K'$.

The functions \mathcal{P} can be therefore calculated *exactly* using an appropriate Gauss integration formula with a small number of points. On the other hand, the functions $F_{p, q}$ entering the tri-dimensional integral (5) are very complicated functions of the variables z, x, μ . Therefore, the integral (5) requires the use of extended and dense integration grids (about $(1000)^3$ points) so as to yield the needed accuracy. Since, the same integration has to be repeated for each ν, ν' , the complete calculation of $\mathcal{W}_{\nu, \nu'}$ could be very time consuming.

However, the function $\mathcal{P}_{p, q}(z, x, \mu)$ can be written in general as

$$\mathcal{P}_{p, q}(z, x, \mu) = \mathcal{P}_{p, q}^e(z, x, \mu) + \sqrt{1+x} \sqrt{1-z^2} \mathcal{P}_{p, q}^o(z, x, \mu), \quad (8)$$

where $\mathcal{P}_{p, q}^e$ and $\mathcal{P}_{p, q}^o$ are polynomials in z, x and μ of maximum degree $N = K + K' + 2$, the 2 coming (eventually) from the factor r_{ij}^2 multiplying the tensor operators in Eq. (4). More precisely \mathcal{P}^e ($\sqrt{1+x}\sqrt{1-z^2}\mathcal{P}^o$) is the even (odd) part of \mathcal{P} with respect to the variable μ .

Now, if $p(t)$ is a polynomial of degree n with respect to the variable t and its value in each of $n+1$ points t_1, \dots, t_{n+1} is known, using the following ‘‘Lagrange interpolation’’ formula, $p(t)$ can be computed *exactly* for any t :

$$p(t) = \sum_{i=1, \dots, n+1} p(t_i) L_i^{(n+1)}(t), \quad L_i^{(n+1)}(t) \equiv \prod_{j=1, \dots, n+1, j \neq i} \frac{t - t_j}{t_i - t_j}. \quad (9)$$

Therefore, once three sets of points z_1, \dots, z_{N+1} , x_1, \dots, x_{N+1} and μ_1, \dots, μ_{N+1} in the interval $(-1, 1)$ have been selected, and $\mathcal{P}_{p, q}^{e, o}$ in the $(N+1)^3$ points z_i, x_j, μ_k have been computed, the functions $\mathcal{P}_{p, q}$ are then known *exactly* for all possible values of (z, x, μ) . Since the matrix elements of the 3N interaction are needed only between HH states with $K \lesssim 30$ (and therefore $\max[N] \ll 100$), as discussed in Sec. IV D, this means that in practice the functions \mathcal{P} have to be evaluated only a fairly small number of times. Finally, if we evaluate

$$I_{i, j, k}^{p, q} = \int_{-1}^1 dz \sqrt{1+z} \int_{-1}^1 dx \sqrt{1-x^2} \int_{-1}^1 d\mu F_{p, q}(r_{12}, r_{13}, \mu_{12, 13}) \times \\ \times L_i^{(N+1)}(z) L_j^{(N+1)}(x) L_k^{(N+1)}(\mu), \quad (10)$$

$$J_{i, j, k}^{p, q} = \int_{-1}^1 dz \sqrt{1+z} \int_{-1}^1 dx \sqrt{1-x^2} \int_{-1}^1 d\mu F_{p, q}(r_{12}, r_{13}, \mu_{12, 13}) \times \\ \times \sqrt{1+x} \sqrt{1-z^2} L_i^{(N+1)}(z) L_j^{(N+1)}(x) L_k^{(N+1)}(\mu), \quad (11)$$

the required matrix elements can be obtained simply as

$$\mathcal{W}_{\nu, \nu'}(\rho) = \sum_{p, q} \sum_{i, j, k=1}^N \left[\mathcal{P}_{p, q}^e(z_i, x_j, \mu_k) I_{i, j, k}^{p, q} + \mathcal{P}_{p, q}^o(z_i, x_j, \mu_k) J_{i, j, k}^{p, q} \right]. \quad (12)$$

where the integrals given in Eqs. (10) and (11) do not depend any more on the quantum numbers ν, ν' of the HH states and therefore can be computed with the necessary accuracy once and for all and stored on computer disks. In this way, the matrix elements $\mathcal{W}_{\nu,\nu'}(\rho)$ obtained via Eq. (12) are obtained very quickly (with only $\sim (N+1)^3$ operations).

-
- [1] H. Kamada *et al.*, Phys. Rev. C **64**, 044001 (2001)
 - [2] B. S. Pudliner *et al.*, Phys. Rev. C **56**, 1720 (1997)
 - [3] A. Nogga, H. Kamada, W. Glöckle, Phys. Rev. Lett. **85**, 944 (2000).
 - [4] R. B. Wiringa, S. C. Pieper, J. Carlson, and V. R. Pandharipande, Phys. Rev. C **62**, 014001 (2000).
 - [5] R. B. Wiringa, V. G. J. Stoks, and R. Schiavilla, Phys. Rev. C **51**, 38 (1995).
 - [6] V. G. J. Stoks *et al.*, Phys. Rev. C **49**, 2950 (1994)
 - [7] R. Machleidt, F. Sammarruca and Y. Song, Phys. Rev. C **53**, R1483 (1996)
 - [8] R. Machleidt, Phys. Rev. C **63**, 024001 (2001)
 - [9] P. Doleshall and I. Borbély, Phys. Rev. C **62**, 054004 (2000)
 - [10] P. Doleshall *et al.*, Phys. Rev. C **67**, 064005 (2003)
 - [11] S. A. Coon *et al.*, Nucl. Phys. **A317**, 242 (1979)
 - [12] H.T. Coelho, T.K. Das and M.R. Robilotta, Phys. Rev. C **28**, 1812 (1983)
 - [13] S. Weinberg, Phys. Lett. B **251**, 288 (1990)
 - [14] U. van Kolck, Phys. Rev. C **49**, 2932 (1994)
 - [15] E. Epelbaum, W. Glöckle, and Ulf-G. Meissner, Nucl. Phys. **A671**, 295 (2000); see also [arXiv:nucl-th/0405048](#) and reference therein.
 - [16] O. Yakubovsky, Sov. J. Nucl. Phys. **5**, 937 (1967).
 - [17] H. Kamada, W. Glöckle, Nucl. Phys. **A 548**, 205 (1992); W. Glöckle, H. Kamada, Phys. Rev. Lett. **71**, 971 (1993).
 - [18] N. W. Schellingerhout, J.J. Schut and L. P. Kok, Phys. Rev. C **46**, 1192
 - [19] J. Carlson, Phys. Rev. C **38**, 1879, (1988).
 - [20] K. Varga and Y. Suzuki, Phys. Rev. C **52**, 2885 (1995).
 - [21] Y. Suzuki and K. Varga, *Stochastic variational approach to quantum mechanical few-body problems*, Springer-Verlag, 1998.
 - [22] H. Kameyama, Kamimura, and Y. Fukushima, Phys. Rev. C **40**, 974 (1989).
 - [23] M. Kamimura and H. Kameyama, Nucl. Phys. **A508**, 17c (1990).
 - [24] P. Navrátil and B. R. Barrett, Phys. Rev. C **59**, 1906 (1999).
 - [25] P. Navrátil, J. P. Vary and B. R. Barrett, Phys. Rev. Lett. **84**, 5728 (2000); Phys. Rev. C **62**, 054311 (2000).
 - [26] N. Barnea, W. Leidemann, G. Orlandini, Phys. Rev. C **61**, 054001 (2000)
 - [27] A. Kievsky, S. Rosati, and M. Viviani, Nucl. Phys. **A577**, 511 (1994).
 - [28] M. Viviani, A. Kievsky, and S. Rosati, Nucl. Phys. **A737**, 205c (2004).
 - [29] M. Viviani, A. Kievsky, and S. Rosati, Few-Body Systems **18**, 25 (1995).
 - [30] M. Viviani, S. Rosati, and A. Kievsky, Phys. Rev. Lett. **81**, 1580 (1998).
 - [31] M. Viviani *et al.*, Phys. Rev. Lett. **86**, 3739 (2001).
 - [32] V. F. Demin, Yu. E. Pokrovsky, and V.D. Efros, Phys. Lett. **44B**, 227 (1973)
 - [33] B. A. Fomin and V. D. Efros, Sov. J. Nucl. Phys. **34**, 327 (1981); Phys. Lett. **98B**, 389 (1981).
 - [34] J. L. Ballot, Few-Body Systems Suppl. **1**, ed. Ciofi degli Atti, O. Benhar, E. Pace and G. Salmé (Springer Verlag, Wien 1987), p 140;
 - [35] J. L. Ballot, Z. Phys. A **302**, 347 (1981)
 - [36] V. D. Efros, Sov. J. Nucl. Phys. **15**, 128 (1972); *ibid.* **27**, 448 (1979)
 - [37] V. F. Demin, Sov. J. Nucl. Phys. **26**, 379 (1977)
 - [38] M. Fabre de la Ripelle, Ann. Phys. (N.Y.) **147**, 281 (1983)
 - [39] T. R. Schneider, Phys. Lett. **40B**, 439 (1972)
 - [40] M.S. Kildushov, Sov. J. Nucl. Phys. **16** (1973) 117
 - [41] V.D. Efros, Sov. J. Nucl. Phys. **30** (1979) 43; B.A. Fomin and V.D. Efros, Sov. J. Nucl. Phys. **34** (1981) 327
 - [42] A. Novoselsky and J. Katriel, Phys. Rev. **A49** (1994) 833; Ann. Phys. **256** (1997) 192
 - [43] L.Deng, D. Li, Y. Wang and C.Deng, Phys. Rev. C **51** (1995) 163
 - [44] V.D. Efros, Few-Body Systems **19** (1995) 167
 - [45] M. Viviani, Few-Body Systems **25**, 177 (1998).
 - [46] A. Kievsky, L.E. Marcucci, S. Rosati and M. Viviani, Few-Body Systems, **22** (1997) 1
 - [47] F. Zernike and H.C. Brinkman, Proc. Kon. Ned. Acad. Wensch. **33**, 3 (1935)
 - [48] R. A. Malfliet and J. A. Tjon, Nucl. Phys. **A217** (1969) 161
 - [49] B. N. Zakharyev, V. V. Pustovalov and E. D. Efros, Sov. J. Nucl. Phys. **8**, 234 (1969)
 - [50] M. Viviani, A. Kievsky and S. Rosati, Il Nuovo Cimento **105 A**, 1473 (1992)
 - [51] A. Nogga *et al.*, Phys. Rev. C **65**, 054003 (2002).
 - [52] K. Varga, private communications (please note that the SVM result reported in Ref. [20] in Table V has been probably

computed with a different version of the ATs3 potential).

- [53] Y. Akaishi, *International Review of Nuclear Physics*, (World Scientific, Singapore, 1986), Vol. 4, p. 259.
- [54] R. Lazauskas and J. Carbonell, private communication.
- [55] A. B. Volkov, Nucl. Phys. **74**, 33 (1965)
- [56] I. R. Afnan and Y. C. Tang, Phys. Rev. **175**, 1337 (1968)
- [57] D. R. Thompson, M. LeMere and Y. C. Tang, Nucl. Phys. **A286**, 53 (1977)
- [58] S. A. Sofianos *et al.*, Phys. Rev. C **26**, 228 (1982)
- [59] V. G. J. Stoks *et al.*, Phys. Rev. C **48**, 792 (1993)
- [60] J. L. Friar, D. Hüber and U. van Kolck, Phys. Rev. C **59**, 53 (1999)
- [61] D. H. Beck and R. D. McKeown, Ann. Rev. Nucl. Part. Sci. **51**, 189 (2001) ([hep-ph/0102334](#))
- [62] Jefferson Lab. proposal E00-114, “Parity Violation from ^4He at Low Q^2 : A Clean Measurement of ρ_s ”, accepted by PAC 18, D. S. Armstrong and R. Michaels spokepersons (HAPPEX collaboration) (web page: <http://hallaweb.jlab.org/experiment/HAPPEX/>).
- [63] S. Ramavataram, E. Hadjimichael and T. W. Donnelly, Phys. Rev. C **50**, 1175 (1994)
- [64] A. Bohr and B. R. Mottelson, *Nuclear Structure*. Vol. I (Benjamin, New York, 1969)
- [65] N. Barnea *et al.*, [arXiv:nucl-th/0404086](#)
- [66] A. Nogga *et al.*, Phys. Rev. C **67**, 034004 (2003)
- [67] N. K. Timofeyuk, Nucl. Phys. **A632**, 19 (1998) and references therein
- [68] S. K. Adhikari *et al.*, Phys. Rev. C **50**, 822 (1994)
- [69] B. C. Karp *et al.*, Phys. Rev. Lett. **53**, 1619 (1984); Nucl. Phys. **A457**, 15 (1986)
- [70] F. Merz *et al.*, Phys. Lett. B **183**, 144 (1987)
- [71] H. R. Weller *et al.*, Phys. Rev. C **34**, 32 (1986)
- [72] M. Viviani, A. Kievsky and S. Rosati, in preparation
- [73] S. Rosati, M. Viviani, and A. Kievsky, Few-Body Systems Suppl. **8**, 21 (1995)
- [74] J. Carlson, V. R. Pandharipande, and R. B. Wiringa, Nucl. Phys. A **401**, 59 (1983)

TABLE I: Number of four-nucleon antisymmetrical hyperspherical-spin-isospin states for the case $J = 0$, $T = 0$ and $\pi = +$ and the selected values of the grandangular quantum number K and total angular momentum L . M_{KL} is the total number of the states defined in Eq. (2.10). M'_{KL} gives the number of the linearly independent states with $\ell_1 + \ell_2 + \ell_3 \leq 6$. See the text for details.

K	$L = 0$		$L = 1$		$L = 2$	
	M_{KL}	M'_{KL}	M_{KL}	M'_{KL}	M_{KL}	M'_{KL}
0	2	1				
2	10	1	9	1	6	1
4	30	4	45	4	30	3
6	70	8	135	12	89	9
8	140	14	315	27	205	18
10	252	24	630	54	405	36
12	420	41	1,134	96	721	63
14	660	59	1,890	160	1,190	102
16	990	90	2,970	250	1,854	158
18	1,430	128	4,455	375	2,760	236
20	2,002	176	6,435	488	3,960	321
22	2,730	235	9,009	585	5,511	385
24	3,640	282	12,285	675	7,475	445
30	3,876		9,180		16,540	
40	10,626		26,565		47,145	
50	23,751		61,425		107,900	

TABLE II: Quantum numbers of the first channels considered in the expansion of the α -particle WF. See the text for details.

α	ℓ_1	ℓ_2	ℓ_3	L_2	L	S_a	S_b	S	T_a	T_b	T
1	0	0	0	0	0	1	1/2	0	0	1/2	0
2	0	0	0	0	0	0	1/2	0	1	1/2	0
3	0	0	2	0	2	1	3/2	2	0	1/2	0
4	1	1	0	0	0	1	1/2	0	0	1/2	0
5	1	1	0	0	0	0	1/2	0	1	1/2	0
6	1	1	0	1	1	1	1/2	1	0	1/2	0
7	1	1	0	1	1	1	3/2	1	0	1/2	0
8	1	1	0	1	1	0	1/2	1	1	1/2	0
9	0	2	0	2	2	1	3/2	2	0	1/2	0
10	2	0	0	2	2	1	3/2	2	0	1/2	0
11	1	1	0	2	2	1	3/2	2	0	1/2	0
12	1	0	1	1	0	1	1/2	0	1	1/2	0
13	1	0	1	1	0	0	1/2	0	0	1/2	0
14	0	1	1	1	0	1	1/2	0	1	1/2	0
15	0	1	1	1	0	0	1/2	0	0	1/2	0
16	1	0	1	1	1	1	1/2	1	1	1/2	0
17	1	0	1	1	1	1	3/2	1	1	1/2	0
18	1	0	1	1	1	0	1/2	1	0	1/2	0
19	0	1	1	1	1	1	1/2	1	1	1/2	0
20	0	1	1	1	1	1	3/2	1	1	1/2	0
21	0	1	1	1	1	0	1/2	1	0	1/2	0
22	1	0	1	1	2	1	3/2	2	1	1/2	0
23	0	1	1	1	2	1	3/2	2	1	1/2	0

TABLE III: Convergence of α -particle binding energies (MeV) corresponding to the inclusion in the WF of the different classes C1-C6 in which the HH basis has been subdivided.

K_1	K_2	K_3	K_4	K_5	K_6	MT-V	AV18	AV18+UIX
20						28.928	14.701	14.902
30						29.794	15.992	16.162
40						29.962	16.172	16.337
50						30.008	16.205	16.369
60						30.024	16.213	16.377
70						30.032	16.214	16.379
72						30.033	16.214	16.379
72	8					30.714	18.286	18.985
72	16					31.170	19.755	20.645
72	24					31.240	19.967	20.865
72	32					31.256	20.014	20.909
72	36					31.259	20.022	20.916
72	40					31.261	20.026	20.919
72	40	8				31.300	21.940	24.682
72	40	16				31.336	23.237	27.142
72	40	24				31.340	23.371	27.350
72	40	30				31.341	23.385	27.370
72	40	34				31.341	23.388	27.373
72	40	34	8			31.341	23.525	27.553
72	40	34	16			31.344	24.086	28.312
72	40	34	20			31.346	24.145	28.382
72	40	34	24			31.347	24.163	28.404
72	40	34	28			31.347	24.170	28.414
72	40	34	28	16			24.181	28.427
72	40	34	28	20			24.191	28.439
72	40	34	28	24			24.195	28.444
72	40	34	28	24	4		24.205	28.456
72	40	34	28	24	8		24.209	28.461
72	40	34	28	24	12		24.210	28.462
“exact”						31.360	24.25	28.50

TABLE IV: Increments of the α -particle BE $\bar{\Delta}(K)$, computed using Eqs. (4.5) for the various classes $i = 1, \dots, 6$ and the MT-V and AV18 potential models. The quantities $c(K, p)$ are defined in Eq. (4.4) and $(\Delta B)_i$, given by $c(k, p)\bar{\Delta}_i(K)$, represents the “missing BE” for having truncated the expansion over the class i up to the given value of $K = K_M$. Finally, the “total missing BE” $(\Delta B)_T$ is computed from Eq. (4.6).

i	K_M	MT-V			AV18		
		$\bar{\Delta}_i(K)$ [keV]	$c(K, 5)$	$(\Delta B)_i$ [keV]	$\bar{\Delta}_i(K)$ [keV]	$c(K, 7)$	$(\Delta B)_i$ [keV]
1	72	0.89	8.51	7.57	0.10	5.52	0.55
2	40	0.71	4.52	3.21	0.91	2.86	2.60
3	34	0.07	3.77	0.26	1.16	2.37	2.75
4	28	0.13	3.03	0.39	2.30	1.87	4.30
5	24	-	-	-	1.47	1.54	2.26
$(\Delta B)_T$				11.43	12.46		

TABLE V: The α -particle binding energies B (MeV), rms radii (fm) and expectation value $\langle K \rangle$ of the kinetic energy operator (MeV) for various central interaction models as computed by means of the HH expansion are compared with the results obtained by other techniques. The binding energies obtained by using the extrapolation technique described in Sect. IV A are enclosed in parentheses.

Interaction	Method	B	$\langle r^2 \rangle^{1/2}$	$\langle K \rangle$
Volkov	HH (this work)	30.420	1.490	50.319
	SVM [20]	30.42	1.49	
	HH [35]	30.399		
ATS3	HH (this work)	31.618	1.412	74.366
	SVM [52]	31.616	1.42	
Minnesota	HH (this work)	29.947	1.4105	58.086
	SVM [20]	29.937	1.41	
	EIHH [26]	29.96	1.4106	
MT-V	HH (this work)	31.347(31.358)	1.4081	69.792
	SVM [20]	31.360	1.4087	
	EIHH [26]	31.358	1.40851	
	CRCG [23]	31.357		
	FY [17]	31.36		
	ATMS [53]	31.36	1.40	
MT-I/III	HH (this work)	30.310(30.331)	1.4380	66.180
	FY [18]	30.312		

TABLE VI: The α -particle binding energies B (MeV), the rms radii (fm), the expectation values of the kinetic energy operator $\langle K \rangle$ (MeV), and the P and D probabilities (%) for various realistic interaction models as computed by means of the HH expansion are compared with the results obtained by other techniques. The binding energies obtained by using the extrapolation technique described in Sect. IV A are enclosed in parentheses.

Interaction	Method	B	$\langle r^2 \rangle^{1/2}$	$\langle K \rangle$	P_P	P_D
AV18	HH (this work)	24.210(24.222)	97.84	1.512	0.347	13.74
	FY [51]	24.25	97.80		0.35	13.78
	FY [54]	24.223	97.77	1.516		
Nijm II	HH (this work)	24.419(24.432)	100.27	1.504	0.334	13.37
	FY [51]	24.56	100.31			
AV18+UIX	HH (this work)	28.462(28.474)	113.30	1.428	0.73	16.03
	FY [51]	28.50	113.21		0.75	16.03
	GFMC [4]	28.34(4)	110.7(7)	1.44		
AV18+TM'	HH (this work)	28.301(28.313)	110.27	1.435	0.73	15.63
	FY [51]	28.36	110.14		0.75	15.67

TABLE VII: Percentages of the total isospin components $T = 1$ and 2 in the α -particle ground states for various interaction models.

interaction	method	$P_{T=1}$ [%]	$P_{T=2}$ [%]
AV18	HH this work	$2.8 \cdot 10^{-3}$	$5.2 \cdot 10^{-3}$
AV18	FY [51]	$3 \cdot 10^{-3}$	$5 \cdot 10^{-3}$
Nijm-II	HH this work	$1.6 \cdot 10^{-3}$	$7.4 \cdot 10^{-3}$
AV18+UIX	HH this work	$2.5 \cdot 10^{-4}$	$5.0 \cdot 10^{-3}$

TABLE VIII: Effect of the inclusion of the various isospin mixing terms in the nuclear Hamiltonian on the percentages of the total isospin components $T = 1$ and 2 in the α -particle ground states. The calculations have been performed using the AV18 model for the nuclear Hamiltonian. For the explanation of the various terms H_{IC} , etc, see the text.

interaction	$P_{T=1}$ [%]	$P_{T=2}$ [%]
H_{IC}	0	0
$H_{IC} + H_C$	$1.5 \cdot 10^{-3}$	$0.1 \cdot 10^{-3}$
$H_{IC} + H_C + H_{CSB}$	$3.0 \cdot 10^{-3}$	$4.9 \cdot 10^{-3}$
$H_{IC} + H_C + H_{CSB} + H_{em}$	$2.8 \cdot 10^{-3}$	$5.2 \cdot 10^{-3}$

TABLE IX: Effects of the truncation of the NN potential when acting only on pairs having total angular momentum $j \leq j_M$. The potential model chosen is the AV18 and the selected HH basis has $\{K_1, K_2, K_3, K_4, K_5, K_6\} = \{64, 40, 34, 24, 0, 0\}$.

j_M	B (MeV)	T (MeV)	P_P (%)	P_D (%)
4	-24.124	97.692	0.344	13.713
6	-24.161	97.771	0.345	13.724
8	-24.164	97.773	0.345	13.725
10	-24.165	97.773	0.345	13.725
20	-24.163	97.774	0.345	13.720
∞	-24.163	97.774	0.345	13.720

TABLE X: Effects of the truncation of the 3N potential when acting only on four-body HH states of grand angular quantum number $K \leq K_M$. The potential model chosen is the AV18+UIX and the selected HH basis has $\{K_1, K_2, K_3, K_4, K_5, K_6\} = \{64, 40, 34, 0, 0, 0\}$.

K_M	B (MeV)	T (MeV)	P_P (%)	P_D (%)
20	27.351	109.71	0.596	15.05
24	27.366	109.67	0.596	15.05
30	27.372	109.65	0.596	15.05
34	27.374	109.64	0.596	15.05

TABLE XI: ANC's and the parameter D_2^{dd} obtained with the HH expansion and the solution of the differential equation of Eq. (4.32) for two potential models. The D_2 parameter is defined in Eq. (4.40). In the third row, the theoretical estimate for D_2^{dd} of Ref. [68] is also shown. Finally, in the last three rows, some available experimental value for the parameter D_2^{dd} have been also reported.

Parameter	C_S^{pt}	C_S^{mh}	C_S^{dd}	C_D^{dd}	D_2^{dd} (fm ²)
AV18	1.72	1.67	1.96	-0.209	-0.115
AV18+UIX	1.75	1.69	1.99	-0.277	-0.113
Adhikari <i>et al.</i> [68]					-0.12
Karp <i>et al.</i> [69]					-0.3 ± 0.1
Merz <i>et al.</i> [70]					-0.19 ± 0.04
Weller <i>et al.</i> [71]					-0.2 ± 0.05

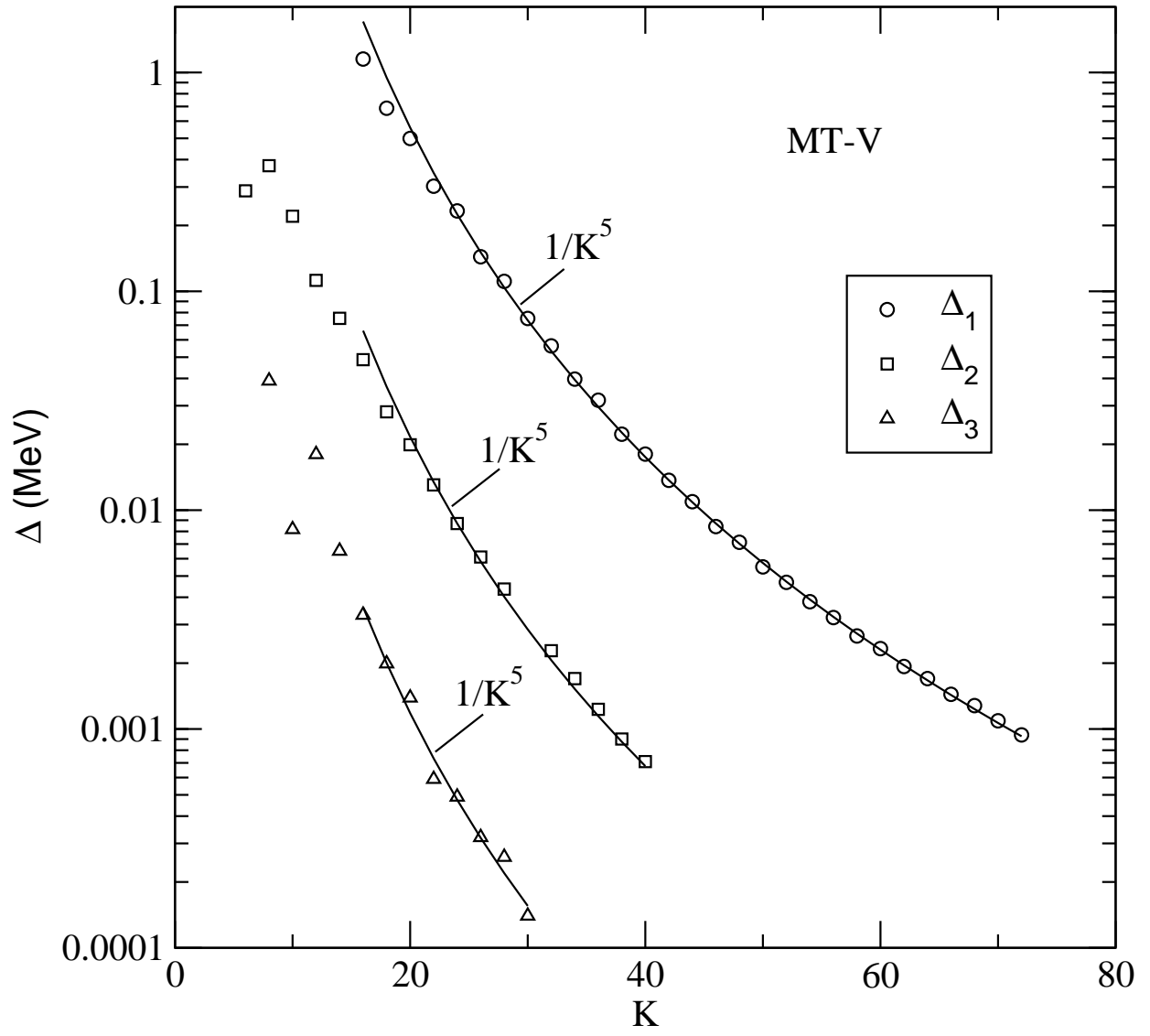


FIG. 1: Binding energy differences for the α particle for the classes C1 (circles) C2 (squares) and C3 (up triangles) as function of the grand angular value K (see the text for more details). The potential used is the MT-V. The curves are fitted to the large K part of the energy differences.

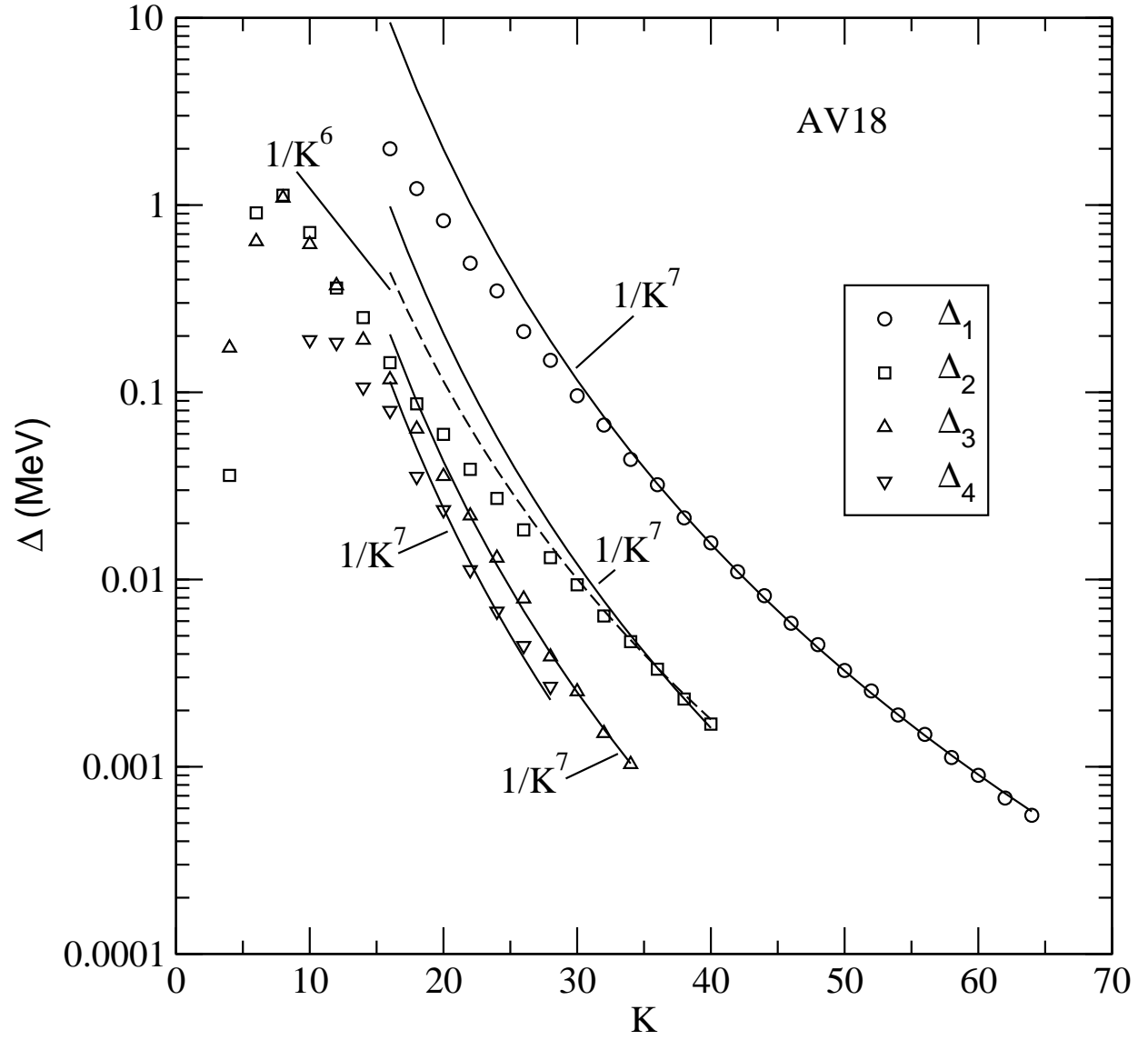


FIG. 2: Binding energy differences for the α particles for the classes C1 (circles) C2 (squares), C3 (up triangles) and C4 (down triangles) as function of the grand angular value K (see the text for more details). The potential used is the AV18. The curves are fitted to the large K part of the energy differences.

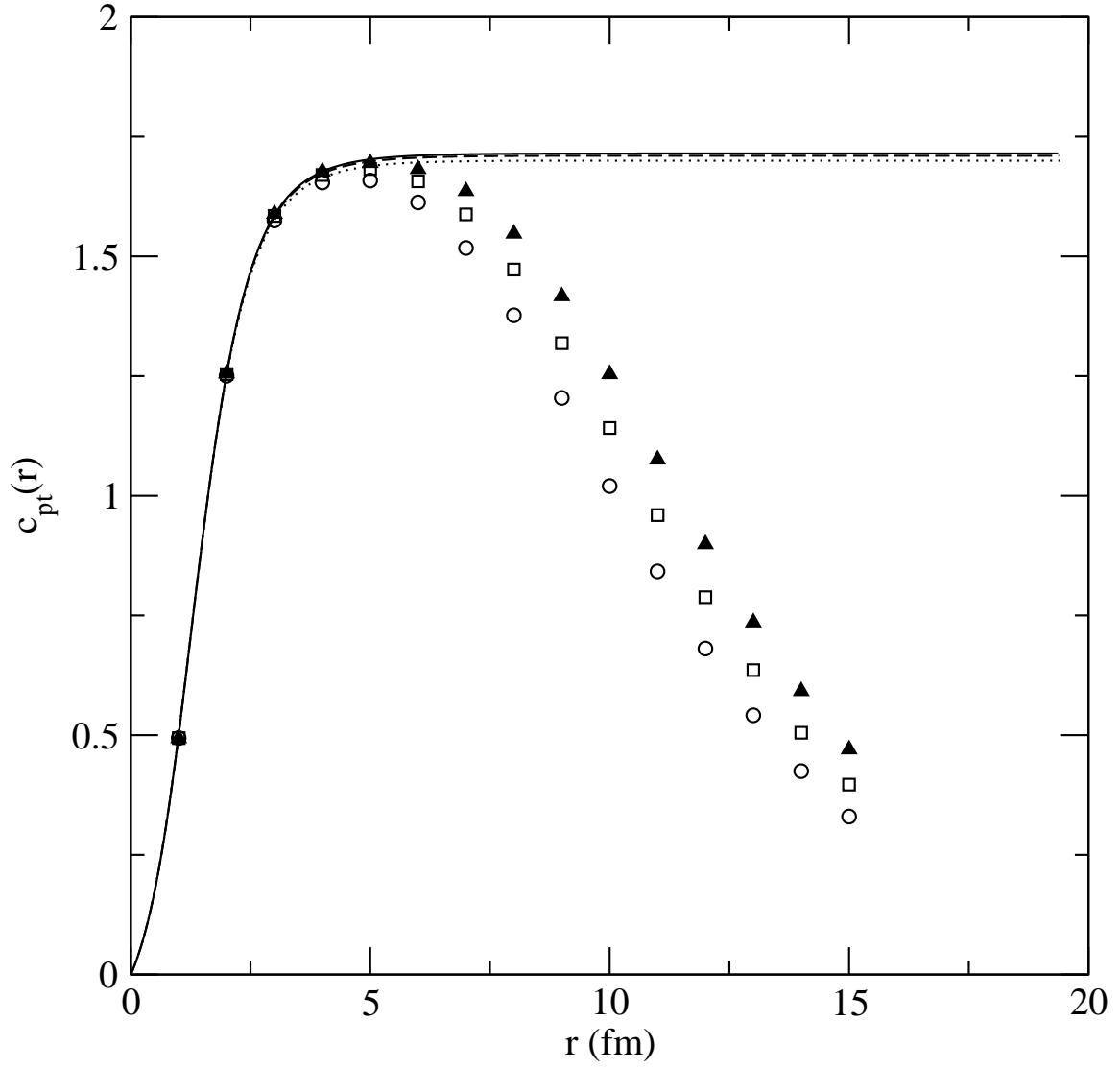


FIG. 3: Ratios $c_{pt}(r_{pt})$ as function of the $p - {}^3\text{H}$ distance r_{pt} . The ratios obtained by the direct calculation of the overlap defined in Eq. (4.28) with the ${}^4\text{He}$ WF corresponding to the gran angular quantum numbers specified in Eq. (4.31) are shown by the open circles (case a), the open squares (case b) and the solid triangles (case c). The ratios obtained by the solution of the differential equation defined in Eq. (4.32) are shown by the dotted (case a), dashed (case b) and solid lines (case c), respectively (the dashed and solid line are almost coincident). The ${}^4\text{He}$ WF were generated using the AV18 potential.

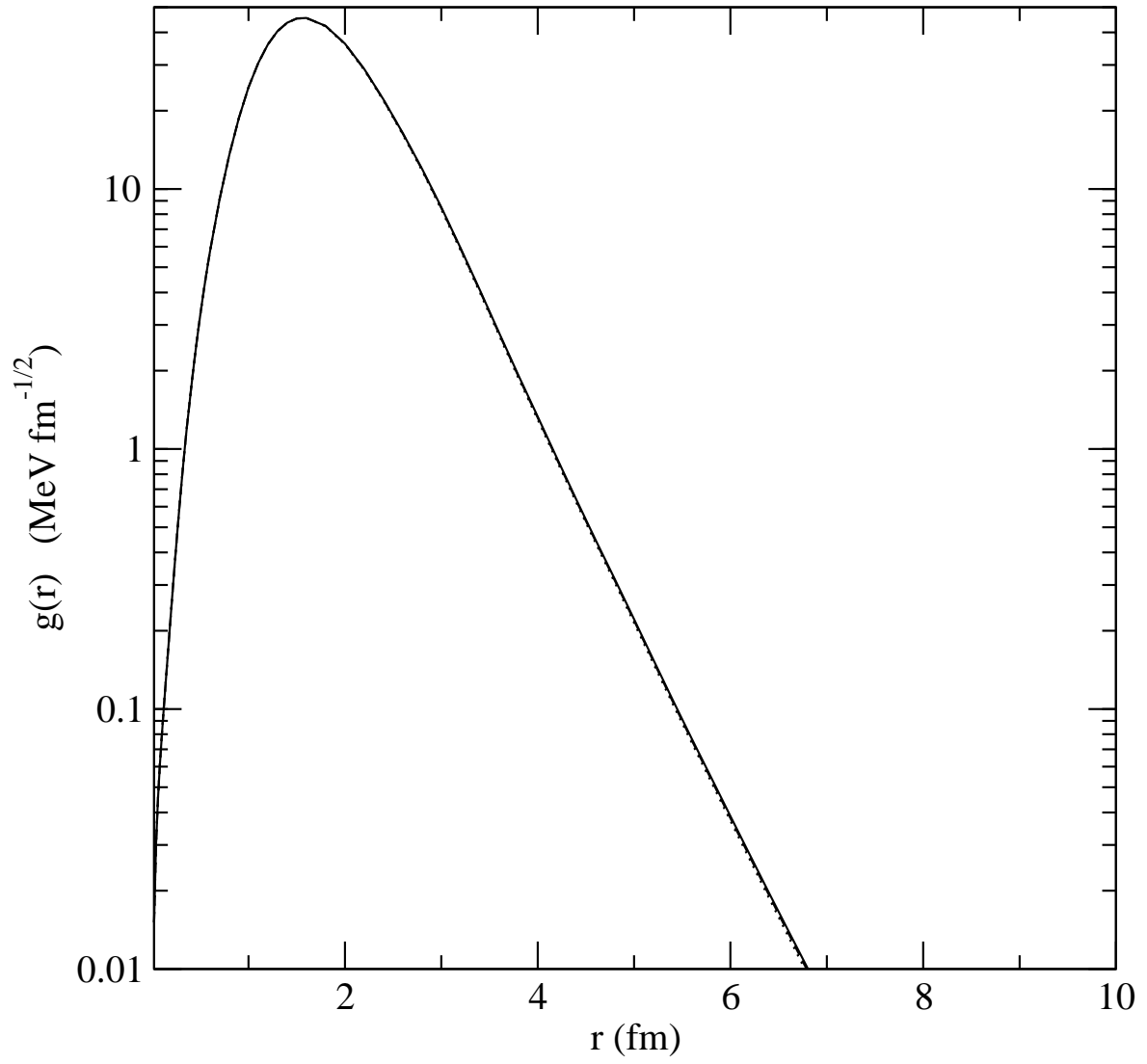


FIG. 4: Functions $g(r)$ obtained for three choices of the HH basis specified in Eq. (4.31) are shown by the dotted (case a), dashed (case b) and solid lines (case c). The three lines are practically coincident and cannot be distinguished.